Published online May 17, 2018

Special Section: Stable Isotope Approaches in Vadose Zone Research

Core Ideas

- To determine the water retention curve from inverse modeling, θ and ψ need to be monitored.
- $\delta^{18}O$ ratios contained information to inversely estimate soil hydraulic parameters.
- Different observation types should be combined in a single OF to estimate parameters.
- Averages of local measurement could be described using effective parameters.
- Accurate measurement of fluxes at lysimeter boundaries improved model parameterization.

J. Groh, A. Lücke, T. Pütz, J. Vanderborght, and H. Vereecken, Institute of Bio- and Geoscience: Agrosphere (IBG-3), Forschungszentrum Jülich GmbH, Jülich, Germany; J. Groh, Research Area 1 Landscape Functioning, Working Group Hydropedology, Leibniz Centre for Agricultural Landscape Research (ZALF), Müncheberg, Germany; C. Stumpp, Institute of Groundwater Ecology, Helmholtz Zentrum München GmbH, Neuherberg, Germany, and Institute of Hydraulics and Rural Water Management, Univ. of Natural Resources and Life Sciences, Vienna, Austria. *Corresponding author (j.groh@fz-juelich.de).

Received 12 Sept. 2017.
Accepted 3 Apr. 2018.
Supplemental material online.

Citation: Groh, J., C. Stumpp, A. Lücke, T. Pütz, J. Vanderborght, and H. Vereecken. 2018. Inverse estimation of soil hydraulic and transport parameters of layered soils from water stable isotope and lysimeter data. Vadose Zone J. 17:170168. doi:10.2136/vzj2017.09.0168

Inverse Estimation of Soil Hydraulic and Transport Parameters of Layered Soils from Water Stable Isotope and Lysimeter Data

Jannis Groh,* Christine Stumpp, Andreas Lücke, Thomas Pütz, Jan Vanderborght, and Harry Vereecken

Accurate estimates of soil hydraulic parameters and dispersivities are crucial to simulate water flow and solute transport in terrestrial systems, particularly in the vadose zone. However, parameters obtained from inverse modeling can be ambiguous when identifying multiple parameters simultaneously and when boundary conditions are not well known. Here, we performed an inverse modeling study in which we estimated soil hydraulic parameters and dispersivities of layered soils from soil water content, matric potential, and stable water isotope ($\delta^{18}O$) measurements in weighable lysimeter systems. We used different optimization strategies to investigate which observation types are necessary for simultaneously estimating soil hydraulic and solute transport parameters. Combining water content, matric potential, and tracer (e.g., $\delta^{18}O$) data in one objective function (OF) was found to be the best strategy for estimating parameters that can simulate all observed water flow and solute transport variables. A sequential optimization, in which first an OF with only water flow variables and subsequently an OF with transport variables was optimized, performed slightly worse indicating that transport variables contained additional information for estimating soil hydraulic parameters. Hydraulic parameters that were obtained from optimizing OFs that used either water contents or matric potential could not predict non-measured water flow variables. When a bromide (Br^-) tracer experiment was simulated using the optimized parameters, the arrival time of the bromide pulse was underestimated. This suggested that Br^- sorbed onto clay minerals and amorphous oxides under the prevailing geochemical conditions with low pH values. When accounting for anion adsorption in the simulation, Br^- concentrations were well predicted, which validated the dispersivity parameterization.

Abbreviations: 2SOS, two-step optimization strategy; AV-NSE, average Nash–Sutcliffe efficiency; BOS Bi-objective optimization strategy; BTC, breakthrough curve; D_L, longitudinal dispersivity; ET, actual evapotranspiration; LAI, leaf area index; MOS, multi-objective optimization strategy; NSE, Nash–Sutcliffe efficiency; OF, objective function; SCEM, Shuffled Complex Evolution Metropolis; δ^2H, stable isotope ratio of $^2H/^1H$; $\delta^{18}O$, stable isotope ratio of $^{18}O/^{16}O$.

Quantification of water fluxes and fluxes of dissolved substances in the vadose zone is important to resolve a number of environmental issues. These issues comprise (i) the protection of groundwater resources, which is the main source of drinking water in many regions of the world (Aeschbach-Hertig and Gleeson, 2012; Taylor et al., 2013), both in terms of groundwater quantity and quality, and (ii) optimizing crop production by making efficient use of water, fertilizers, and plant protection products. Simulation models are used to link known fluxes at the upper boundary of the vadose zone with fluxes at different depths in the vadose zone and related state variables such as water contents, matric potentials, and solute concentrations. These simulation models require accurate and precise information about the properties of the vadose zone that link fluxes with state variables, such as the soil water retention curve, the unsaturated soil hydraulic conductivity, and the solute dispersion coefficient. Typically, these properties are determined from laboratory experiments, and the precision of the estimated properties has increased considerably during the last decade by improving the experimental and estimation

procedures (Peters and Durner, 2006, 2008; Peters et al., 2015). However, these laboratory-scale estimated properties may have low accuracy describing field-scale processes due to spatial variability at the field scale, which is not captured by limited sampling; small sampling volumes (e.g., soil cores or columns) subjected to specific boundary conditions that differ from real world conditions; and scale-dependent solute transport parameters (Hopmans et al., 2013). The inability of laboratory scale determined soil hydraulic and solute transport parameters to describe field and larger scale water flow and transport processes under natural conditions is an issue in many hydrological applications (Mertens et al., 2005; Wöhling et al., 2008; Iiyama, 2016).

In situ observations of state variables and fluxes at the scale of interest and inverse modeling have been shown to be promising approaches to estimate soil hydraulic parameters (Peters and Durner 2006; Puhlmann and von Wilpert, 2012; Stumpp et al., 2012; Ries et al., 2015; Sprenger et al., 2015). However, inverse modeling requires the specification of boundary (e.g., actual evapotranspiration, drainage flux, and capillary rise) and initial conditions (e.g., water content, matric potential, and solute concentration), which are often not available or associated with large uncertainties in outdoor experiments (Vrugt et al., 2008; Li et al., 2009; Mannschatz and Dietrich, 2017). For example, various studies have shown that standard devices to measure precipitation (tipping bucket) frequently underestimate the amount of rain (Gebler et al., 2015; Groh et al., 2015; Hoffmann et al., 2016; Herbrich et al., 2017) and affect the estimation of soil hydraulic properties (Peters-Lidard et al., 2008). Also, boundary conditions at the bottom of the soil profile can have an important impact on the water fluxes and state variables within the investigated system (Groh et al., 2016) and hence need to be correctly represented. In the past, mainly free-drainage (zero-gradient) or a seepage-face boundary were used in inverse modeling studies. The latter boundary condition can be applied to lysimeters with a seepage face at the bottom across which water and solutes can leave the soil profile when the seepage face is saturated with water. Although this boundary condition can be accurately represented in the simulation model, water and solute fluxes observed from lysimeters with a seepage face at the bottom are not representative of field-scale conditions (Flury et al., 1999; Boesten, 2007; Kasteel et al., 2007). Breaking the capillary connection between the soil profile and deeper soil layers affects drainage, the movement of solutes, and evapotranspiration and prevents capillary rise (Schwaerzel and Bohl, 2003; Abdou and Flury, 2004; Stenitzer and Fank, 2007). Alternatively, time series of state variables, for example matric potential, could be used as a bottom boundary condition. However, this leads to a loss of information because the temporal evolution of the state variable is not used to derive information about the system properties but is prescribed as a boundary condition.

The majority of field-scale inverse modeling studies have used solely information about water content (e.g., Qu et al., 2014; Fang et al., 2015; Seki et al., 2015; Lai and Ren, 2016; Le Bourgeois et al., 2016). However, because water fluxes in the soil are driven by gradients in matric potential, in situ observations of water content do not necessarily provide sufficient information to accurately parameterize the field-scale hydraulic properties (Vereecken et al., 2008; Scharnagl et al., 2011; Wöhling and Vrugt, 2011). When aiming at inversely estimating transport parameters, concentrations of artificial or environmental tracers can be used. Particularly water stable isotopes have been shown to give information about water transit times and dispersivities (Stumpp et al., 2012; Sprenger et al., 2015; Stockinger et al., 2015, 2016).

Surprisingly little attention has been given to combining different observation types to calibrate water flow and transport models. In some studies, soil hydraulic parameters and/or longitudinal dispersivity were estimated from inverse modeling using a combination of in situ observation variables, e.g., water content and matric potential (Wöhling and Vrugt, 2011; Caldwell et al., 2013; Groh et al., 2013), water content and evapotranspiration data (Foolad et al., 2017), water content and $\delta^{18}O$ isotope ratio profiles (no continuous monitoring; Sprenger et al., 2015, 2016a), deuterium-enriched water (Stumpp et al., 2009), or Br^- (Abbasi et al., 2003). Only a few studies were found that used a combination of water content, solute concentration, and matric potential (Mishra and Parker, 1989; Jacques et al., 2002; Stumpp et al., 2012). Soil layering, which corresponds to the vertical variation of soil properties, is often not considered when estimating hydraulic and transport parameters using inverse modeling, and it is assumed that the soil profile can be represented by a homogenous profile with one set of effective parameters. Such an effective approach can be used to describe averaged state variables and fluxes when hydraulic properties are described by random space functions. However, when soil layers are relatively thick compared with the soil profile depth that is considered in simulations and when the properties of the layers vary considerably, the vertical variation in soil properties cannot be represented by a random space function but is rather a deterministic variation. In such a case, homogenous effective parameters are of little meaning to describe the vertical variation of state variables and fluxes. This implies that the properties of the different layers need to be determined.

Schelle et al. (2012) showed, using synthetic data, that soil-layer-specific observations of state variables, e.g., matric potentials, were prerequisite to inversely determine soil hydraulic parameters of different layers in a layered soil profile. Stumpp et al. (2012) and Jacques et al. (2002) used a stepwise and sequential approach to derive parameters layer by layer to avoid non-uniqueness of parameter estimates when a larger number of parameters had to be estimated. However, this approach ignored possible parameter interaction between corresponding soil layers (Wöhling and Vrugt, 2011). Hence, simultaneous estimation of the full parameter set for a layered soil using various observation types including water content, matric potential, and water isotope data is therefore promising. Because tracer concentrations depend also on water flow and root water uptake, these measurements constrain parameters not only for solute transport but also for water flow and root water uptake (Sprenger et al., 2015). Mishra and Parker (1989) used a

synthetic data set of a simple infiltration–evaporation scenario to demonstrate that the information on water content, matric potential, and solute concentration at the corresponding soil layer was beneficial to identify simultaneous layer-specific soil hydraulic and solute transport properties. However, no systematic verification was conducted within their numerical study, and thus it is still unclear which variables are necessary to adequately describe soil hydraulic properties as well as the transport behavior of layered soils in outdoor experiments under variable boundary conditions.

Using state-of-the-art weighable lysimeter systems can help overcome the above-mentioned limitations at the field scale because all relevant surface and bottom boundary water fluxes can be determined with a high temporal resolution and high precision (von Unold and Fank, 2008). Hence, lysimeters equipped with matric potential and soil water content sensors and devices for soil water sampling are ideal experimental systems to obtain high-resolution observation data for the inverse estimation of water flow and solute transport parameters under realistic transient boundary conditions (Schelle et al., 2013). However, observations of state variables within the lysimeters at a specific depth are still local measurements (Garré et al., 2011; Cai et al., 2016), raising the question to what extent such local observations are representative for a given depth within the lysimeter. Our hypothesis is that the average value of several local measurements from one depth in several lysimeters can be used to derive a layer-specific effective parameterization and help to identify soil hydraulic properties and dispersivities that describe water and matter fluxes at the field scale.

In this framework, our study compared different inverse modeling strategies (stepwise and simultaneous) including the use of water stable isotope data to identify soil hydraulic and solute transport properties of a layered soil profile. The software HYDRUS-1D (Šimůnek et al., 2016) was used to simulate water and solute fluxes, and a global optimization algorithm was used to calibrate the vadose zone model.

Different inverse modeling strategies were used: (i) to investigate which state variables are necessary to estimate soil hydraulic properties as well as the solute transport parameter (dispersivity) of a layered soil; (ii) to identify effective hydraulic properties and longitudinal dispersivities of a layered soil using horizontally averaged state variables from four large-scale lysimeters; and (iii) to use Br^- concentrations from an artificial tracer experiment to validate the calibrated dispersivity parameters of the vadose zone model.

Materials and Methods

Study Site Wüstebach

The experimental site Wüstebach (50°30′10″ N, 6°19′41″ E, 630 m asl) is located within the Eifel National Park and is part of the Lower Rhine Valley–Eifel observatory of TERENO and the Germany-wide lysimeter network SOILCan (Bogena et al., 2015; Pütz et al., 2016). The vegetation cover and plant growth on the lysimeter and the surrounding area correspond to a forest meadow with no agricultural activities (Knauer et al., 2017). The area belongs to the humid temperate climate zone, with a mean annual precipitation of 1200 mm and a mean annual temperature of 7.5°C (Pütz et al., 2016). Since December 2010, six weighable lysimeters (Wu4– Wu9, METER Group), each with a surface of 1 m^2 and a depth of 1.5 m, were installed at the research test site. The Wüstebach catchment is covered with a 1- to 3-m-thick periglacial solifluction layer, and the bedrock is fractured Devonian shale and sandstone (Rosenbaum et al., 2012). The cylindrical lysimeters contain undisturbed soil monoliths of a Stagnic Cambisol, which is the dominant soil type in the western part of the Wüstebach catchment. The soil was described and soil samples were taken from two soil profiles during the lysimeter excavation process (see Table 1). The profiles were taken beside (southeast and northwest) the lysimeter excavation location and showed a similar layering. Only the soil texture of the fourth layer differed significantly (southeast: sand > 75%; northwest: loam > 69%).

The lysimeters are located annularly around a central service pit, which houses the measurement equipment and data recording devices. The lysimeters have a tension-controlled bottom boundary system that adjusts the matric potential at the 1.4-m depth in the lysimeter to measured matric potentials (TS1 tensiometer, METER Group) at the same depth in the field. Hence, we can assume that water and solute fluxes in the lysimeter are directly transferable to the surrounding field. Each lysimeter was equipped with tensiometers (TS1, METER Group), time domain

Table 1. Soil analysis from two profiles in Wüstebach (southeast and northwest), which were taken beside the lysimeter excavation location. Stone content was estimated according to Ad Hoc Arbeitsgruppe Boden (2005). The depths of the northwest profile were used to define the model layers. Layers II Bv 1 and II Bv 2 were grouped into one model layer.

Soil horizon		Layer depth		Texture (sand/silt/clay)		Stone content	
Southeast	Northwest	Southeast	Northwest	Southeast	Northwest	Southeast	Northwest
		m		%			
Of, Oh	Of, Oh	+0.02–0	+0.02–0	–	–	–	–
Ah–Sew	Ah	0–0.21	0–0.15	40/28/32	35/24/41	0	20
II Bv 1	Sew–Ssw	0.22–0.43	0.16–0.31	61/18/21	47/19/34	30	20
II Bv 2	II Bv 1	0.44–0.68	0.32–0.59	81/13/6	22/70/8	40	20
II Bv 3	II Bv 2	0.69–1.00	0.59–1.10	75/17/8	23/69/8	50	50
III Cv	III Cv	1.01–1.50	1.11–1.50	64/17/19	65/17/18	70	80

reflectometry probes (CS610, Campbell Scientific), and suction cups (SIC20, METER Group) at the 0.10-, 0.30-, 0.50-, 1.40- or 1.45-m soil depth. The weighing precision is 10 g (≅0.01 mm) for the lysimeter and 1 g (≅0.001 mm) for the water reservoir tank in which the effluent from a lysimeter is collected and from which water is pumped back into the lysimeter during periods of upward flow at the bottom of the lysimeter. Weight measurements are logged every minute. Further information about the general design and setup of the SOILCan lysimeter network were provided by Pütz et al. (2016).

Lysimeter weight changes are not related only to water storage changes because these are also affected by external factors like management operations, animals, or wind. The separation of precipitation and evapotranspiration from lysimeter weight changes thus requires an appropriate data processing scheme to reduce the impact of external errors and noise on the calculation of water fluxes (Schrader et al., 2013; Hannes et al., 2015). The raw data of lysimeter measurements were subjected to extensive manual (visually, software DIAdem, National Instruments) and automated plausibility checks to ensure the quality of the observation dataset (for more details, see Pütz et al., 2016; Küpper et al., 2017). Subsequently, the Adaptive Window and Adaptive Threshold filter (Peters et al., 2017) was used to further smooth the noise-prone lysimeter weight changes. Daily precipitation and evapotranspiration amounts were calculated from the smoothed lysimeter signal. We assumed that any increase or decrease in mass during a 1-min time period can be related to precipitation or actual evapotranspiration, respectively. Meteorological parameters were used to calculate the hourly potential evapotranspiration of a hypothetical grass surface with the Penman–Monteith equation (Allen et al., 1998). To capture the seasonal vegetation development, measurements of grass length and leaf area index (LAI) were conducted with a measuring stick and an LAI-2200 plant canopy analyzer (LI-COR).

The salt tracer experiment started on 4 Dec. 2013. On each of five lysimeters (Lys-Wu4 and Lys-Wu6–Lys-Wu9) ~1 L of KBr solution (~25 g Br^-) was sprayed followed by 0.5 L of pure water for flushing the application device. Lysimeter Lys-Wu5 received no Br^- and was used as a reference. We used a frame to avoid Br^- loss during the application because of wind drift. The inner side of the frame was covered (per lysimeter) with aluminum foil to collect splashing tracer water. The loss of Br^- due to splashing was determined in the laboratory. After tracer application on the corresponding lysimeter and flushing, the application device was washed; water was collect and analyzed in the laboratory. The setup guarantees recalculation of the exact amount of Br^- applied to each lysimeter. The amount of applied Br^- was 25.08 g for Lys-Wu4, 24.83 g for Lys-Wu6, and 25.30 g for Lys-Wu8. We did not measure $\delta^{18}O$ ratios in Lys-Wu7 and Lys-Wu9; hence measurements of Br^- concentrations and water fluxes from Lys-Wu7 and Lys-Wu9 were not part of this study. Because a tracer solution enriched in δ^2H was applied to Lys-Wu8, we used the $\delta^{18}O$ ratio as a tracer in our investigation since more comparable time series were available for this isotope.

Soil water samples from suction cups at the 0.1-, 0.3-, and 0.5-m depth and from the seepage water (1.45 m) were collected every 2 wk. At the beginning of the tracer experiment and after heavy rainfall events (> ~30 mm d^{-1}), water samples were collected weekly or twice a week. Since December 2013, soil water samples were analyzed for $\delta^{18}O$, δ^2H, and Br^- for Lys-Wu4, Lys-Wu5, Lys-Wu6, and Lys-Wu8. Precipitation samples were collected during the observation period from January 2012 to April 2016 with a wet deposition collector (cooled) and sampled weekly. The isotopic analysis was performed with a laser-based cavity ring-down spectrometer (L2130-i analyzer, Picarro). Isotope values are given in δ notation relative to the Vienna Standard Mean Ocean Water (V-SMOW). The measurement accuracy was ≤0.1‰ for $\delta^{18}O$ and ≤1.0‰ for δ^2H. The Br^- concentrations of the soil water samples were determined with an ion chromatography system (ICS-3000, Dionex, Thermo Fisher Scientific), which had a relative measurement error of 3.2% for concentrations ≥0.5 μg mL^{-1}.

Model Setup

Water Flow

The one-dimensional water flow model HYDRUS-1D (Šimůnek et al., 2016), which numerically solves the Richards equation, was used to simulate transient water flow in the lysimeters. The Mualem–van Genuchten model (van Genuchten, 1980) was selected to describe the water retention characteristic $\theta(h)$ and the unsaturated hydraulic conductivity function $K(h)$:

$$\theta(h)=\begin{cases}\theta_r+\dfrac{\theta_s-\theta_r}{\left(1+|\alpha h|^n\right)^m} & h<0\\ \theta_s & h\geq 0\end{cases} \quad [1]$$

$$K(h)=K_s\left(\frac{\theta-\theta_r}{\theta_s-\theta_r}\right)^{\tau}\left\{1-\left[1-\left(\frac{\theta-\theta_r}{\theta_s-\theta_r}\right)^{1/m}\right]^m\right\}^2 \quad [2]$$

where θ, θ_s, and θ_r are the actual, saturated, and residual volumetric water contents [L^3 L^{-3}], respectively; α [L^{-1}] is related to the reciprocal of the air-entry value, n (dimensionless) to the width of the pore size distribution, $m = 1 - 1/n$, τ (dimensionless) is the pore connectivity parameter, and K_s is the saturated hydraulic conductivity [L T^{-1}].

The upper boundary condition was defined as a time-dependent atmospheric boundary with surface runoff. The actual evapotranspiration, measured from the corresponding lysimeter, was used as a boundary condition instead of the potential evapotranspiration to further constrain the parameter estimates. We set the parameter of hCritA, which describes the minimum allowed matric potential at the soil surface, to a value of -10^8 cm. This value guarantees that the actual evaporation rate was decreased from the potential value only during extreme dry conditions (matric potential < -10^8 cm). No reduction of actual transpiration due to plant water stress was observed in the grassland

lysimeter under the relatively wet climate conditions. The actual evaporation and transpiration were calculated from actual evapotranspiration according to Beer's law using LAI and the canopy radiation extinction constant (0.463) for the partitioning. The seasonal development of the forest meadow LAI per lysimeter was approximated by a linear interpolation of the LAI measurements. The root water uptake was simulated using the model of Feddes et al. (1978) with the vegetation-specific stress response function for grass, which is available in the HYDRUS-1D software (Šimůnek et al., 2013). The root water uptake was restricted until the maximum rooting depth of 0.6 m, which was determined during the soil profile sampling. Root water uptake decreased linearly between 0.05 m and the maximum rooting depth, were it reached zero. To account for a delay in infiltration during times with snow in the catchment area, a simple approach according to Jarvis (1994) was used. The snowmelt and sublimation constant were set to 0.43 cm d^{-1} $°C^{-1}$ and 0.06, respectively.

Isotope Transport

The solute transport of $\delta^{18}O$ was calculated with the advection–dispersion equation, which is the most widely used model to predict solute transport under transient natural boundary conditions (Vanderborght and Vereecken, 2007). The dispersion coefficient in the advection–dispersion equation represents hydromechanical dispersion, which corresponds with the product of the longitudinal dispersivity D_L [L] and the pore water velocity [$L\ T^{-1}$], and the effective molecular diffusion, which depends on the molecular diffusion in water [$L\ T^{-1}$], and a dimensionless tortuosity factor that is <1 and decreases with decreasing water content.

A modified version of HYDRUS-1D (Stumpp et al., 2012; Šimůnek et al., 2016) was used to simulate the transport of stable isotopes. The module neglects fractionation processes due to evaporation and was successfully applied in various studies (Huang et al., 2015; Sprenger et al., 2015, 2016a, 2016b). The modified code prevents an accumulation of isotopes (equivalent to an increase in isotope ratios) at the soil surface when evaporation occurs and assumes passive uptake by roots, so that water and tracer ($\delta^{18}O$) can leave the system via evaporation and transpiration. The solute transport boundary conditions at the top boundary were described as a time-variable solute flux boundary (Cauchy boundary) when water flow was directed into the system (precipitation) and by a zero concentration gradient (Neumann boundary) when water flux was out of the system (evaporation). At the bottom boundary, a zero concentration gradient (Neumann boundary) was used when the water flux left and entered the system.

Data Used for Boundary and Initial Conditions

The simulated time period was from 1 Jan. 2012 to 30 Apr. 2016. For this period, isotope ratios in the precipitation were available and daily precipitation, evapotranspiration, discharge, and upward directed water flow were derived from lysimeter and effluent reservoir weights. Measurements of internal states of the lysimeters (water contents, water potentials, and $\delta^{18}O$ ratios) were available for a shorter period from 4 Dec. 2013 to 30 Apr. 2016. Therefore, initial conditions for the water flow and isotope transport simulations had to be estimated, and a spin-up phase of 703 d was considered to minimize the effect of the chosen initial conditions on the calibration of the model parameters against measurements of the internal states of the lysimeters. A linear decrease of pressure head between the top (−70 cm) and the bottom boundary nodes (−50 cm) was chosen as an initial condition for water flow. The initial $\delta^{18}O$ ratios in the soil profile were estimated by averaging the measured $\delta^{18}O$ ratios derived from the soil water samples at the 0.1- and 1.45-m depths throughout the entire observation period. We assumed a linear decrease of the $\delta^{18}O$ ratios between the top and bottom of the soil profile; please note that all isotope values were transferred into positive numbers by adding an arbitrary value for the simulation only because it is not possible to use negative numbers in the modeling procedure.

Definition of Soil Layers in the Simulation Model

Figure 1 shows both soil profiles, the position of the measurement devices, and the conceptual representation of the layering in HYDRUS-1D for all four lysimeters. The layering of both profiles was rather similar; hence the conceptual representation of the

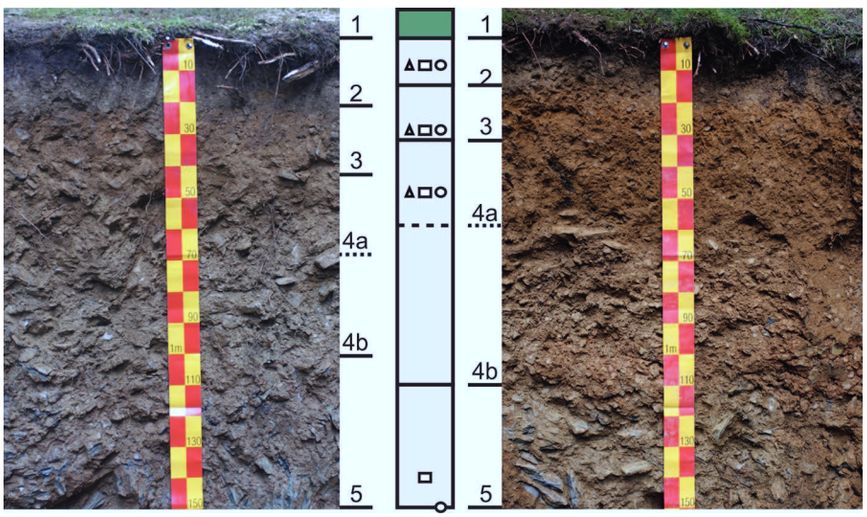

Fig. 1. The two soil profiles from the Wüstebach catchment (southeast [left] and northwest [right]), the conceptual representation of the layering in the HYDRUS-1D simulation (which was based on the northwest profile), and the positions of the measurement devices and observation points in the simulation. The locations of the measurement devices are: time domain reflectometry probes (triangles), tensiometers (rectangles), and suction cups (circles).

layering in the simulation was based on the northwest profile. In total, seven parameters had to be estimated or optimized for four soil horizons to simulate the water (θ_r, θ_s, α, n, K_S, and τ) and solute transport (D_L). The lysimeters at Wüstebach were covered with a few-centimeters-thick moss layer. Previous studies showed that internal water fluxes in mosses affect the drainage behavior across the moss layer and change the rate of evaporation (Price and Whittington, 2010), as the physiology of moss differs from that of other plants (Suzuki et al., 2007) or bare soil conditions (Blok et al., 2011). To represent moss in our hydrological model, the hydraulic and transport properties of the moss layer were set to θ_r = 0.01 cm^3 cm^{-3}, θ_s = 0.92 cm^3 cm^{-3}, α = 0.4373 cm^{-1}, n = 1.405, K_s = 175 cm d^{-1}, τ = −2.31, and D_L = 5 cm according to McCarter and Price (2014) and Stofberg et al. (2016). The thickness of the moss layer was 0.05 m.

Parameter Optimization and Model Efficiency

To reduce the amount of data, daily averages of matric potentials and water contents were calculated from the measurements. These were compared with daily values of water contents and matric potentials that were simulated by HYDRUS-1D. The $\delta^{18}O$ ratios in the collected effluent from the lysimeter were compared with a flux-weighted average of $\delta^{18}O$ ratios that were simulated in the pore water at the bottom of the lysimeter during the time period that the effluent was collected. The same procedure was used to compare the $\delta^{18}O$ ratios in the pore water with simulated ratios at the depth of the soil water samplers.

Parameter values for θ_s in Layers 2 to 4 were estimated from the measured soil water retention characteristic using RETC (van Genuchten et al., 1991) to reduce the number of optimization parameters. The parameter search space of the water flow and solute transport parameters during the optimization is summarized in Table 2. The lower boundary for the parameter τ was defined according to Peters et al. (2011).

We used the Shuffled Complex Evolution Metropolis algorithm (SCEM; Vrugt et al., 2003) to determine, for each lysimeter and soil layer, the soil hydraulic parameters and the longitudinal dispersivity. The SCEM is a global optimization algorithm that has been applied to a wide range of hydrological problems at different scales (Heimovaara et al., 2004; Raat et al., 2004; Ries et al., 2015). The algorithmic variables that need to be specified are the number of complexes q (e.g., 25 = number of parameters) and the population size s (e.g., $q \times 10$). We considered four different optimization strategies that included different sets of observations:

1. Bi-objective optimization strategy (BOS1): water content and $\delta^{18}O$ data at all available soil depths (0.1, 0.3, 0.5, and 1.45 m) are used to calibrate the soil hydraulic parameters and D_L of the HYDRUS-1D model.
2. Bi-objective optimization strategy (BOS2): matric potential used instead of water content data compared with BOS1.
3. Two-step optimization strategy (2SOS): soil hydraulic parameters were estimated from layer-specific measurements of water content and matric potential in a first optimization run with SCEM. In a next step, the transport parameters D_L were estimated for each soil layer from the $\delta^{18}O$ data using the optimized hydraulic parameters obtained in the first run.
4. Multi-objective optimization strategy (MOS): uses water content, matric potential, and $\delta^{18}O$ ratios simultaneously to calibrate 25 parameters of the advection–dispersion and Richards equations.

Strategies with only one measured state variable (e.g., $\delta^{18}O$ ratios) or pedotransfer functions were not considered because earlier investigations by Sprenger et al. (2015) showed that such a strategy failed to match observations of state variables that were not included in the objective function (water content) during the inverse model calibration. The objective function that was minimized using the SCEM algorithm was based on Nash–Sutcliffe efficiency (NSE). The NSE coefficients were calculated per depth and observation variable to evaluate model behavior and performance:

$$\mathrm{NSE}_{i,v} = 1 - \frac{\sum_t^N \left(x_{v,s,t,i} - x_{v,o,t,i} \right)^2}{\sum_t^N \left(x_{v,o,t,i} - \mu_{v,o,i} \right)^2} \quad [3]$$

where N is the total number of time steps, t is the time step, $x_{v,s,t}$ and $x_{v,o,t}$ are the simulated and observed values of the variable v, and $\mu_{v,o}$ is the mean observed value. The NSE values range between 1 (perfect fit) and $-\infty$. Values below zero imply that the mean of the observations is a better predictor than model simulations. Because the SCEM algorithm minimizes an OF, the average NSE coefficient was defined as NSE − 1. To evaluate and compare among all four strategies, we calculated, based on the optimal parameter set, an average NSE coefficient (AV-NSE) that lumps NSE coefficients for all the observation depths and variables.

No water content measurements were available for Lys-Wu4 in Layer 4 (0.5 m) and for all lysimeters at the 1.4-m depth. At depths where no water content was available, matric potential measurements were used instead of water content in the OF.

Table 2. Lower and upper boundaries of soil hydraulic properties and dispersivity parameter for the inverse parameter optimization strategies. Measured minimum and maximum leaf area index (LAI).

Parameter†	Lower bound	Upper bound
LAI, cm^2 cm^{-2}	0.2	3.7
θ_r, cm^3 cm^{-3}	0	0.36
θ_s, cm^3 cm^{-3}	0.25	0.55
α, cm^{-1}	0.001	0.3
n	1.001	3
K_s, cm d^{-1}	1	1500
τ	$\tau > -2/(1 - 1/n)$	6
D_L, cm	0.1	30

† LAI, leaf area index; θ_r and θ_s, residual and saturated water content, respectively; α and n, shape parameters; K_s, saturated hydraulic conductivity; τ, pore connectivity; D_L, longitudinal dispersivity.

Effective Parameters and Boundary Conditions

Effective Parameters

We used averaged water fluxes at the boundaries of the lysimeters, combined with averaged values of water contents, matric potentials, and $\delta^{18}O$ ratios from the four lysimeters to estimate the effective soil hydraulic parameters and D_L. These parameters were compared with the results for each single lysimeter considering uncertainty caused by parameter equifinality (Beven, 2006). The range of parameter uncertainty was defined as the set of parameter values for which AV-NSE was less than 0.01 smaller than the optimized AV-NSE.

Impact of Precipitation Accuracy on the Simulation of Water and Solute Transport

To quantify as an example the impact of a less accurately defined upper boundary condition on simulated state variables (that is water content, matric potential, and $\delta^{18}O$ ratios), we compared simulations that used daily amounts of precipitation measured with a rain gauge (tipping bucket method) with simulations in which precipitation was derived from the lysimeter weights. When using rain gauge data, the boundary condition for water fluxes at the bottom had to be changed to free drainage (zero gradients) since the measured effluent fluxes in combination with measured evapotranspiration rates and the rain gauge precipitation values led to a long-term decline of stored water in the soil profile. Simulation results for the two cases were compared with measured average water contents, matric potentials, and $\delta^{18}O$ ratios in the four lysimeters.

Validation of Dispersivity Parameters

To validate our soil depth and lysimeter specific dispersivity parameters, we used the optimal parameter set from the best inverse parameter optimization strategy to simulate the Br^- breakthrough curve (BTC) of the conducted tracer experiment in a forward simulation run with HYDRUS-1D. Uptake of Br^- by plants has been reported in various studies (Kung, 1990; Schnabel et al., 1995; Magarian et al., 1998; Xu et al., 2004). We assumed a passive uptake of Br^- by plants during the forward simulations.

Results and Discussion

Lysimeter Observation Data

Table 3 summarizes the precipitation measured by a rain gauge, potential evapotranspiration, and precipitation (P), actual evapotranspiration (ET), discharge, and capillary upflow during the entire observation period (4 Dec. 2013–30 Apr. 2016) derived from lysimeter measurements. Daily surface fluxes (P and ET) derived from lysimeter measurements correlated well with rain gauge measurements and calculated reference ET, respectively (P: $R^2 = 0.7$; ET: $R^2 = 0.83$). However, precipitation sums derived from the lysimeter weights were on average 23% (670 mm) larger than the rain gauge measurements. Because water flow in the soil is driven by precipitation, it is evident that these differences in precipitation estimates will lead to important differences in simulated water fluxes in the soil, which may have an important impact on the calibration of the soil hydraulic and solute transport properties. Similar deviations between standard meteorological precipitation measurement devices (tipping bucket rain gauge) and lysimeters have been reported in the literature (e.g., Groh et al., 2015; Hoffmann et al., 2016; Herbrich et al., 2017). These differences in precipitation between the two methods may be caused by the fact that lysimeters account for the presence of dew, fog, and rime (Gebler et al., 2015). According to Xiao et al. (2009) and Fank and von Unold (2007), dew can be derived from lysimeter mass increase measurements between sunset and sunrise, when rain gauges do not detect precipitation. A threshold of the maximum possible rate of dew formation on clear nights was used (Monteith and Unsworth, 1990) and dew formation rates >0.07 mm h^{-1} were excluded from the analysis. From our measurements, we found that dew formation accounted for ~4.7% of the total lysimeter-derived precipitation, which is in line with previous studies (Xiao et al., 2009; Heusinger and Weber, 2015; Guo et al., 2016) but still explains only a small fraction of the difference in precipitation amounts measured by lysimeters and rain gauges. Weather station exposure or wind effects are another important cause of the underestimation of precipitation by rain gauges (Richter, 1995; Hagenau et al., 2015). The measured cumulative ET was 72% of the calculated reference potential evapotranspiration. This indicates that the stomatal conductance and aerodynamic conductance of the boundary layer above the canopy were smaller than those of the reference crop and/or that evaporation was reduced due to the high insulating capacity of mosses. The variability of daily P, ET, and capillary upflow among the different lysimeters was relatively small and increased with larger daily water fluxes (see Supplemental Fig. S1). However, for drainage, in comparison to the other daily water fluxes, we observed a larger spatial variability (up to ±6 mm d^{-1}), which might be related to the spatial variability of the soil hydraulic properties.

Figure 2 shows the isotopic composition (δ^2H and $\delta^{18}O$) of precipitation and of soil water sampled at different depths from

Table 3. Cumulative water balance components derived from the weather and lysimeter station at the Wüstebach SOILCan test site from 4 Dec. 2013 to 30 Apr. 2016. The reference precipitation and evapotranspiration (ET) corresponds to precipitation derived from a tipping bucket rain gauge and the potential evapotranspiration, respectively.

Lysimeter	Precipitation	ET	Discharge	Capillary rise	Storage change
	mm				
Reference	2337	−1144	–	–	–
Lys-Wu4	2982	−907	−2131	38	−18
Lys-Wu5	3033	−882	−2217	31	−35
Lys-Wu6	3015	−923	−2142	32	−18
Lys-Wu8	2997	−869	−2186	39	−19
Avg.	3007	−895	−2169	34	−23

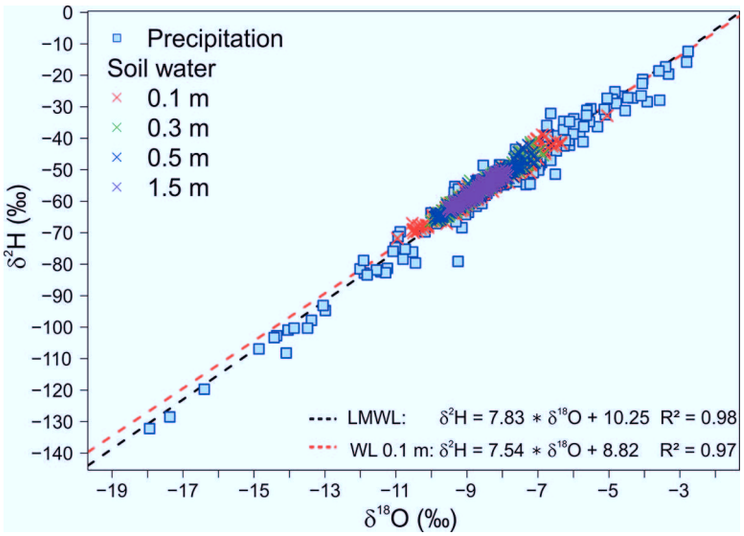

Fig. 2. Isotopic composition of precipitation, soil water from three lysimeters at different soil depths, the local meteoric water line (LMWL), and the water line in the 0.1-m soil depth (WL).

Lys-Wu4, Lys-Wu5, and Lys-Wu6. Stable isotope values in soil water samples from all depths (e.g., the water line [WL] in 0.1 m in Fig. 2) plot close to the local meteoric water line (LMWL), demonstrating no significant impact of fractionation processes due to evaporation or condensation. This implies that the assumption of no fractionation due to evaporation at the soil surface, which we made to define the boundary condition of the isotope transport model, will cause no significant bias between the simulated and measured isotope ratios in the soil. The lack of observable fractionation indicates low evaporation losses from the moss-covered soil surfaces in the wet climate. The high insulating capacity of mosses (low thermal conductivity) can reduce the transfer of energy into the soil (Blok et al., 2011), dew formation decreases water demand from the soil, and consequently, the moss layer restricts evaporation from the ground surface (Suzuki et al., 2007).

Parameter Optimization Strategies

We used the four inverse optimization strategies BOS1, BOS2, 2SOS, and MOS for each lysimeter. The model performance per observation variable (NSE-θ, NSE-ψ, NSE-^{18}O) and AV-NSE efficiency criteria are summarized in Table 4. Additionally, information on the model performance for single-observation variables (NSE$\theta_{,i}$, NSE$\psi_{,i}$, NSE$_{18O,i}$) and depths (i) are provided in Supplemental Table S1. The observed water retention data and the simulated hydraulic conductivity curves, which varied greatly between lysimeters, are shown in Fig. 3 and 4. Further details on the simulated and observed water content, matric potential, and isotope ratios of δ^{18}O are provided in Supplemental Fig. S2, S3, and S4.

Model Performance Using BOS1

The NSE values that were obtained with the BOS1 method for each lysimeter using water content and δ^{18}O ratios ranged between 0.52 and 0.65, −2.06 and 0.31, and −0.15 and 0.37 for water content, matric potential and δ^{18}O data, respectively (Table 4). The smaller NSE-ψ values and the larger deviation between simulated and measured matric potentials (Supplemental Fig. S3) compared with other state variables is obviously the consequence of not including the NSE-ψ values in the OF, as was found in previous studies by Wöhling and Vrugt (2011) and Groh et al. (2013). Hence, water retention functions obtained from BOS1 deviate from field observations (Fig. 3). The simulated hydraulic conductivity varied between the lysimeters and the soil layer (Fig. 4), and the strategy BOS1 achieved an average NSE value of −0.18, which describes the average NSE criterion among all lysimeters (see Lys-average, Table 4).

Model Performance Using BOS2

For BOS2, which used matric potential and δ^{18}O ratios in the OF, measured and simulated matric potential and δ^{18}O ratios agreed well. The NSE-ψ and NSE-^{18}O values varied between 0.12 and 0.56 and between −0.29 and 0.46, respectively. Not including water content measurements in the OF led to large deviations between simulated and observed water contents at several depths (see Supplemental Fig. S2) and consequently to small (very negative) NSE-θ values (−10.69 < NSE-θ < −0.68; Table 4). This might be related to the disequilibrium between measured in situ water contents and matric potentials due to different reaction times of the measuring instrument. According to

Table 4. Simulation results of four different inverse modeling strategies (bi-objective optimization BOS1 and BOS2, two-step optimization 2SOS, and multi-objective optimization MOS). Model performance values are reported aggregated for each observation type: water content (NSE-θ), matric potential (NSE-ψ), and δ^{18}O ratios (NSE-^{18}O); AV-NSE represents model performance for the entire vadose zone and was calculated per lysimeter from single Nash–Sutcliffe efficiency (NSE) values per soil depth and observation type (equally weighted). Additionally NSE per observation type and entire vadose zone that were averaged across the four lysimeters (Lys-average) are reported.

NSE	Lys-Wu4				Lys-Wu5				Lys-Wu6				Lys-Wu8				Lys-average			
observation	BOS1	BOS2	2SOS	MOS	BOS1	BOS2	2SOS	MOS	BOS1	BOS2	2SOS	MOS	BOS1	BOS2	2SOS	MOS	BOS1	BOS2	2SOS	MOS
NSE-θ	0.52	−0.68	0.54	0.52	0.65	−10.69	0.49	0.18	0.65	−2.11	0.53	0.40	0.52	−6.53	0.45	0.42	0.59	−5.00	0.50	0.38
NSE-ψ	0.31	0.37	0.46	0.42	−2.06	0.12	0.09	−0.06	−0.66	0.43	0.24	0.26	−1.24	0.56	0.54	0.49	−0.91	0.37	0.33	0.28
NSE-^{18}O	−0.11	−0.29	−0.97	−0.14	0.20	0.17	0.00	0.09	−0.15	0.17	−0.09	0.01	0.37	0.46	0.39	0.51	0.08	0.13	−0.17	0.12
AV-NSE	0.18	−0.11	−0.10	0.22	−0.50	−2.81	0.16	0.06	−0.11	−0.36	0.20	0.21	−0.30	−1.83	0.48	0.47	−0.18	−1.28	0.19	0.24

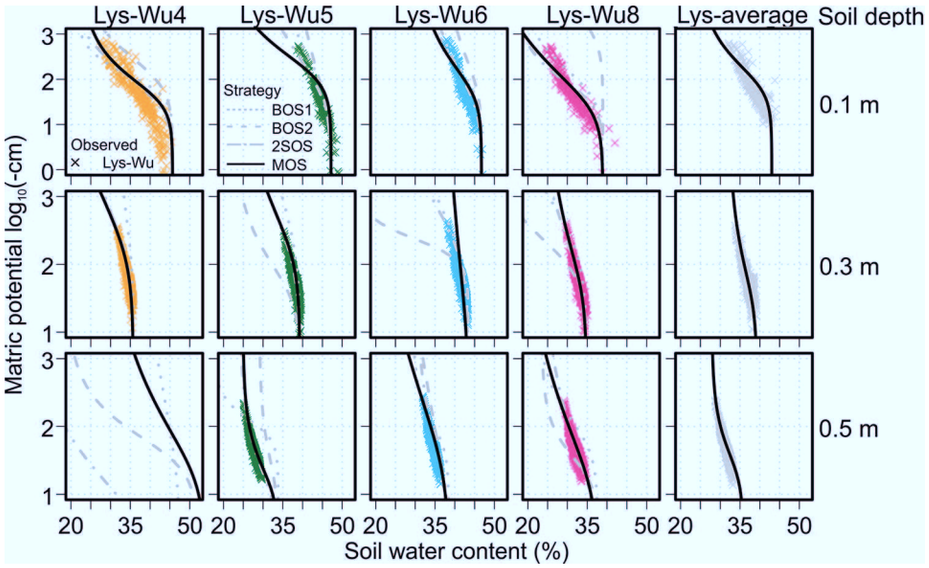

Fig. 3. Observed field water retention data from four different lysimeters (Lys-Wu4, Lys-Wu5, Lys-Wu6, and Lys-Wu8) in three consecutive soil depths and the corresponding water retention curves from four different optimization strategies: bi-objective optimization BOS1 (dotted line) and BOS2 (dashed line), two-step optimization 2SOS (dash-dotted line), and multi-objective optimization MOS (solid line). Additional average field water retention data (Lys-average) and the corresponding effective water retention curve obtained from the MOS strategy are shown.

the average NSE values, not including soil water content data in the OF led to a worse misfit of observations than not including matric potential measurements (average NSE Lys-average BOS2: −1.28). The optimal parameter sets of BOS2 for each lysimeter are listed in Supplemental Table S2 and were for most depths clearly different from values determined by the BOS1 runs. The respective water retention functions yielded less reasonable fits to the observed field water retention data than the results from the BOS1 runs (see, e.g., Lys-Wu5 in 0.5 m in Fig. 3). Also, the parameters of the unsaturated hydraulic conductivity function differed considerably between the two strategies.

The $\delta^{18}O$ ratios were expected to contain some information about the prevailing water contents in the lysimeters because the advective tracer movement is determined by the water flux, which was given as a boundary condition, and the water content in the soil profile. Interestingly, the $\delta^{18}O$ ratios could still be described adequately even when the water contents were off. Because water fluxes that drive the transport of the tracer are only significant

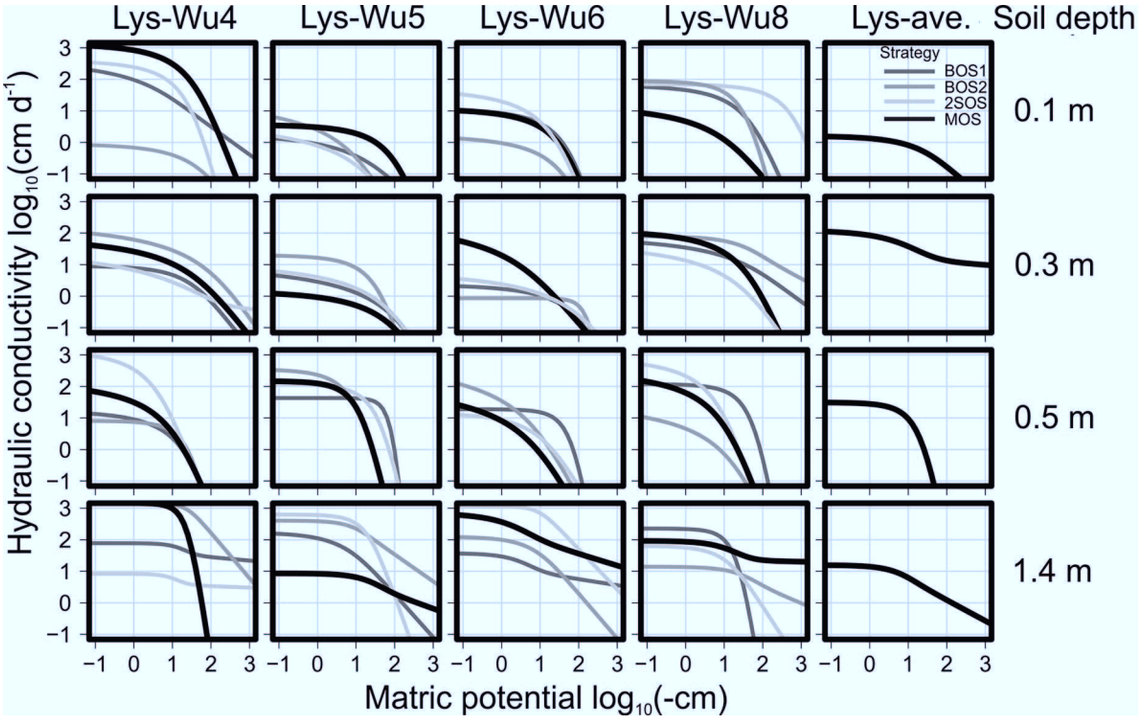

Fig. 4. Simulated hydraulic conductivity curves at 0.1-, 0.3-, 0.5-, and 1.4-m soil depths for lysimeters Lys-Wu4, Lys-Wu5, Lys-Wu6, and Lys-Wu8 from four different optimization strategies: bi-objective optimization BOS1 and BOS2, two-step optimization 2SOS, and multi-objective optimization MOS. Effective simulated hydraulic conductivity curves obtain by the MOS strategy are shown in Lys-average (Lys-ave.).

when the soil is wet, the simulated tracer $\delta^{18}O$ ratios are apparently not influenced by the simulated water conditions under drier soil conditions. However, it must be noted that the small dependence of the tracer transport on the water contents during drier periods is also due to the high precipitation amounts so that the soil is quickly rewetted and transport reactivated after a dry spell, and the timing of the transport is not affected strongly by the antecedent water content. Therefore, time series of $\delta^{18}O$ ratios may be more sensitive to simulated water contents during time periods when water fluxes are insignificant for tracer transport.

Model Performance Using 2SOS

The simulation results from the stepwise strategy 2SOS, which used separate optimization runs to identify soil hydraulic properties based on time series of water content and matric potential and to identify the dispersivity from $\delta^{18}O$ ratios, are summarized in Table 4. The NSE-θ and NSE-ψ values were relative similar to the results for water content from BOS1 and for matric potential from BOS2, respectively. Thus water retention functions derived by strategy 2SOS agreed well with the observed water retention data (see Fig. 3). These findings are in line with previous studies, which showed that a combined use of information during the calibration procedure of water content and matric potential (Abbaspour et al., 2000; Zhang et al., 2003; Wöhling and Vrugt, 2011; Caldwell et al., 2013; Groh et al., 2013) was beneficial for the estimation of soil hydraulic parameters. The estimated parameters of the hydraulic conductivity function with strategy 2SOS differed considerably from BOS1 and BOS2.

Observed topsoil water retention data suggest, at least for Lys-Wu5, Lys-Wu6, and Lys-Wu8, a bimodal pore size distribution. The use of a unimodal water retention function for the simulation led to an underestimation of soil water content in the topsoil for matric potentials below approximately −110 cm. However, the Lys-average NSE-^{18}O value was below zero (−0.17) and thus was clearly lower than that obtained by strategy BOS1 (0.08) or BOS2 (0.13). Simulation results from 2SOS showed a considerable trade-off in fitting both water flow and solute transport parameters with a stepwise strategy. Hence, this suggests that time series of $\delta^{18}O$ ratios contain information content for optimizing not only solute transport but also water flow parameters.

Model Performance Using MOS

The temporal evolution of stable isotopes and scatterplots between simulated and observed time series of water content and matric potential by strategy MOS, which included the three observation types in the OF, are depicted in Supplemental Fig. S2, S3, and S4. The MOS achieved lower NSE-θ but clearly higher NSE-ψ than BOS1 (Table 4). On the other hand, MOS simulations reached notably higher NSE-θ values than BOS2 but lower NSE-ψ values. The NSE-^{18}O values obtained by MOS were nearly identical to the values obtained by BOS1 and BOS2. Comparing simulation results from MOS with 2SOS showed that both strategies achieved rather similar values for NSE-ψ but lower NSE-θ. Water retention functions derived with MOS also matched reasonably well to the observed water retention data. However, MOS obtained higher NSE-^{18}O values than 2SOS (AV-NSE Lys-average MOS: 0.12; 2SOS: −0.17). This suggests that the improved fit of $\delta^{18}O$ ratios when $\delta^{18}O$ ratios, water content, and matric potential measurements were used simultaneously in the optimization strategy resulted in only a small trade-off in the description of the water contents and matric potentials. Identified parameter sets between MOS and 2SOS differed mainly in parameters of the unsaturated hydraulic function and dispersivities (see Supplemental Table S2; Fig. 4). This suggests that $\delta^{18}O$ ratios contain additional information content for optimizing water flow parameters K_s, n, and τ. Hence, the balanced solution MOS achieved, in comparison with all other strategies, the highest average NSE value (Lys-average: 0.24; see Table 4).

A recent simulation study by Sprenger et al. (2015) demonstrated the usefulness of combining soil water content measurements with $\delta^{18}O$ ratio profiles (destructive) to identify layer-wise water flow and solute transport parameters by inverse modeling. Our study supports these findings and demonstrates that a simultaneous instead of a stepwise use of hydrological and hydrochemical data during the parameter optimization procedure increased the model realism and the parameter identifiability. In addition, we showed that expanding the dataset and including matric potentials adds important information that is required to estimate soil hydraulic parameters. Our investigation results imply, for the setup of field hydrological tracer experiments, that water content, matric potential, and water stable isotopes should be measured over time and in several depths to identify more precise estimates of soil hydraulic properties and dispersivities. However, field experiments are often limited by, e.g., budget or time. In this case, it might be important to know which state variable should be monitored. Previous investigations showed that measuring only one state variable (e.g., $\delta^{18}O$ ratios) does not result in sufficient information to parameterize the vadose zone model. Thus, in the case of such limiting conditions in the field, we recommend measuring at least water content and tracer data because the soil water retention characteristic was much better defined by this strategy (BOS1) than by using BOS2.

Effective Parameters and Boundary Conditions

Effective Parameters

The soil hydraulic parameters and the longitudinal dispersivity obtained from MOS varied, some considerably, among the four lysimeters and reflect the spatial heterogeneity of the soil properties at the test site. This heterogeneity was also apparent from the in situ soil texture analysis (Table 1) of two soil profiles located nearby and the spatial variability of the locally observed state variables water content, matric potential, and $\delta^{18}O$ ratio within the lysimeters. The optimal parameters according to the average NSE criterion for the MOS optimization and the range of parameter values that resulted in similar average NSE criteria (average NSE < optimal average NSE + 0.01), which is a relative measure for the

parameter uncertainty (statistical inference about the parameter uncertainty was not performed and would require, for instance, a Bayesian framework), are depicted in Fig. 5. The range of derived K_s values was in line with previous studies at the catchment (Borchardt, 2012; Fang et al., 2016; Wiekenkamp et al., 2016). Relatively high θ_r (up to 0.29) and low K_S values (3.6–15 cm d^{-1}, except for Lys-Wu4) were obtained for the topsoil layers, which had the highest clay content of the soil profile (32–42%). The high θ_r values are in line with the results of Puhlmann and von Wilpert (2012) for forest soils with similar texture. Also, concretions of Fe were visible in the topsoil layers, indicating a high saturation degree and low hydraulic conductivity in the upper soil layer. The parameter uncertainty ranges were, for most soil hydraulic parameters and depths, relatively small and smaller than the range of optimal parameter values in the different lysimeters. This low range indicates that most parameters were sensitive and identifiable. Only for Lys-Wu8 were larger uncertainty ranges obtained for θ_r, K_s, and τ. The pore connectivity parameter τ varied strongly among the lysimeters and differed considerably from the often-used standard value $\tau = 0.5$ (Mualem, 1976). Although negative τ values are physically not feasible because it implies a decrease of tortuosity when the soil dries out, nevertheless various studies have showed negative τ for soils (e.g., Schaap and Leij, 2000; Werisch et al., 2014; Cai et al., 2018) so that τ should be used rather as a shape factor without any physical meaning (Peters et al., 2011). No consistent increase of solute dispersivity with depth was observed, and dispersivity lengths ranging between 3 and 30 cm were in the upper range of the dispersivity lengths that were observed in soil column and field experiments under unsaturated flow conditions (Vanderborght and Vereecken, 2007). The parameter uncertainty range for D_L was especially larger for Lys-Wu6 and Lys-Wu8.

The parameter uncertainty and the variability of parameters obtained in the different lysimeters give rise to two questions. The first is whether our simulation results can predict the spatial variability in state variables that were observed among the different lysimeters. A positive answer to this question implies that the observed spatial variability can be represented by the variability of the optimized soil properties and the variability of the boundary fluxes. A negative answer indicates that other processes or variations in fluxes at a smaller spatial resolution than what is represented by the model and its boundary conditions play an important role for the generation of the observed variability.

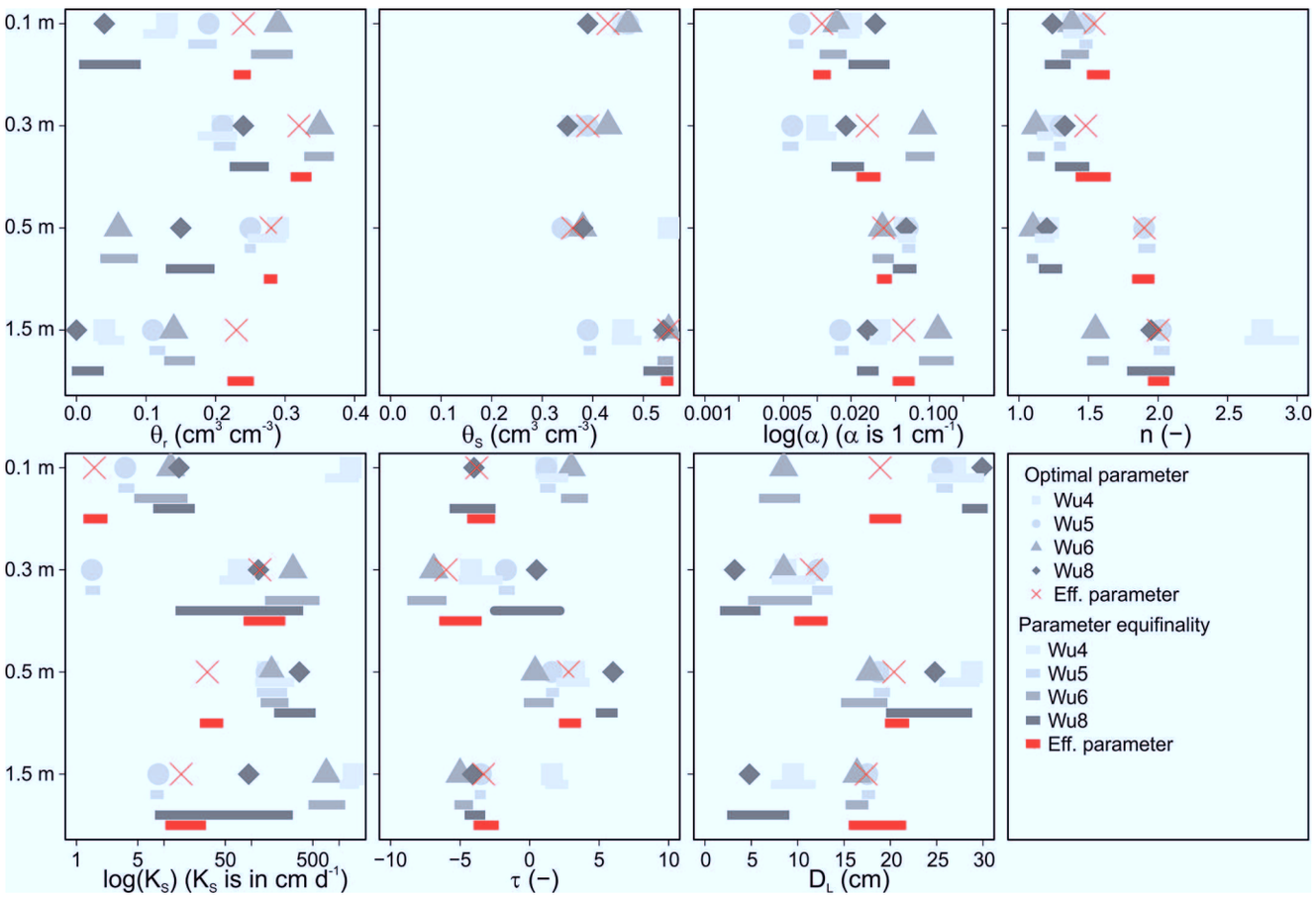

Fig. 5. Best values of the residual and saturated water content (θ_r and θ_s, respectively), shape parameters α and n, saturated hydraulic conductivity (K_s), pore connectivity (τ), and longitudinal dispersivity (D_L) per depth and for each single lysimeter (Lys-Wu4, Lys-Wu5, Lys-Wu6, and Lys-Wu8) and average lysimeter (Eff. parameters) obtained from the multi-objective optimization strategy. Vertical lines represent the parameter uncertainty associated with the parameter equifinality.

Figure 6 plots the coefficient of variation (CV) vs. the spatial mean of the variables at a given soil depth for both the measured and simulated variables. The CVs of the water contents increase with decreasing water content, which is in line with a previous study at the catchment scale at Wüstebach (Korres et al., 2015). Water content at lower depths showed only a slight increase of spatial variability with lower water content, but the CV of 10% is still high. For matric potential, we observed a parabolic shape, with increasing spatial variability during both wetter and drier soil conditions. The lowest spatial variability was around −100 cm in the topsoil and ranged between −40 and −70 and between −24 and −80 cm in the 0.3- and 0.5-m soil depths, respectively. The spatial variability of the simulated matric potentials at 1.4 m increased in the range from −10 to −1 cm (close to saturation) to ∼700%, which was not observed for the measured values. However, the spatial variability in both water content and matric potential was generally well reproduced by the model simulations, indicating that the spatial variability of these state variables could be reproduced using the variability of the estimated soil properties and the boundary conditions. The spatial variability of the optimized parameters might be the reason for the larger observed variability of daily bottom boundary water fluxes among the lysimeters (see Supplemental Fig. S1).

In contrast to the water content and matric potential, the spatial variability of the $\delta^{18}O$ ratios was largely underestimated by the simulations at the 0.1-, 0.3-, and 0.5-m depths. This suggests that model simulations did not account for fast transport paths of tracer within macropores or local variations in water fluxes within the lysimeter. Several investigations showed that not only the model calibration but also the selection of the model itself and the model structure is of high importance because it significantly affects the quality of the simulations (Butts et al., 2004; Crosbie et al., 2011; Gosling et al., 2011; Moeck et al., 2016). Therefore the use of a different model structure that accounts for such fast transport paths (e.g., dual permeability; Gerke and van Genuchten, 1993) and a bimodal soil water retention characteristic (Romano and Nasta,

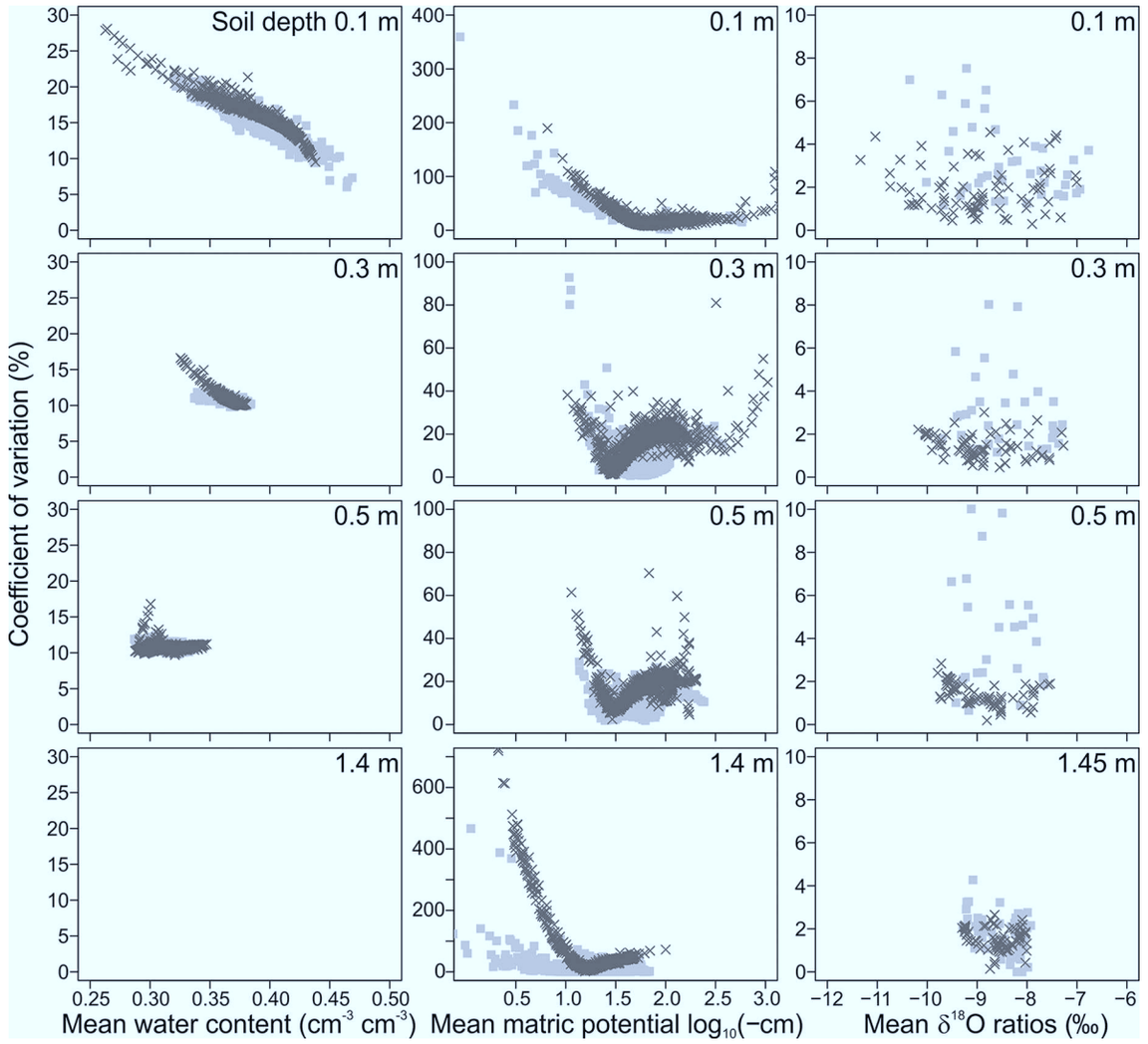

Fig. 6. Coefficient of variation vs. mean water content, matric potential, and $\delta^{18}O$ ratios from field observations (light gray) and model simulations (multi-objective optimization strategy, dark gray) at different depths obtained from four lysimeters.

2016) for the topsoil might have further improved the simulations. However, a more complex model structure like the bimodal water retention function would further increase the number of model parameters in the calibration process. A higher temporal tracer sampling frequency would be needed to detect fast transport paths of water and tracer within macropores and more sampling locations per depth to observe the spatial variability of tracer transport within the lysimeter and to obtain a representative average of the concentrations at a certain depth in the lysimeters (Koestel et al., 2009a, 2009b; Garré et al., 2010).

A second question is whether the effective properties that were used to predict the average water contents, matric potentials, and $\delta^{18}O$ ratios at a given depth at the site differ systematically from the parameters that were obtained for the individual lysimeters. Hence, an additional model calibration run was conducted that optimized the soil hydraulic properties and longitudinal dispersivity using averaged state variables of water content, matric potential, and $\delta^{18}O$ ratio and average boundary fluxes derived from the four lysimeters. The model calibration reached, with respect to NSE-θ, NSE-ψ, and NSE-^{18}O, values of 0.46, 0.33, and 0.02 (Table 5) and thus achieved comparable results to the average model performance in each individual lysimeter (Table 4). Effective parameters are summarized in Supplemental Table S2 and shown in Fig. 3, 4, and 5. We did not observe a systematic difference between the effective parameters and the set of parameters that were obtained for the individual lysimeters. A cross-validation of the calibrated vadose zone model with single lysimeter observations showed that the effective parameter set was able to predict the state variables obtained from the corresponding lysimeter with only a minor reduction of model performance in terms of matric potential and $\delta^{18}O$ ratios, but for water content, NSE values were all below zero. Using a fixed θ_s in the cross-validation from average water retention data caused a partially large offset between simulated and locally observed water content. Still, correlation analysis showed that the dynamic of simulated and observed water content agreed reasonably well (R^2 range >0.45 and <0.70).

Lower Precipitation Accuracy

A less accurately defined atmospheric boundary condition (i.e., precipitation) and bottom boundary (free drainage) and effective parameters obtained by MOS (see Lys-average in Fig. 3 and 4) were used to simulate water content, matric potential, and $\delta^{18}O$ ratio at different measurement locations. The NSE values for the simulation (Rain-gauge) can be taken from Table 5. The NSE values for water content decreased only a little from 0.46 to 0.39, but for matric potential, NSE-ψ showed a strong decrease from 0.33 to −45.57. The low NSE-ψ was mainly related to matric potential simulation in the 1.4-m soil depth. High n and a negative τ value in Layer 5 (Fig. 4) led, in combination with the free-drainage lower boundary, to low simulated matric potentials at the lysimeter bottom. This illustrates clearly that a zero-gradient bottom boundary condition cannot be used to simulate observed water fluxes in the 1.45-m soil depth. For $\delta^{18}O$, an improvement of NSE-^{18}O from 0.02 to 0.31 was achieved. However, results from the simulation run "Lysimeter" captured the time series of simulated $\delta^{18}O$ ratios better than simulations from "Rain-gauge" (see Fig. 7). Particularly, $\delta^{18}O$ ratios in spring and summer did not agree well with observations when using less accurate boundary conditions. Thus, the less pronounced shape of $\delta^{18}O$ ratios in the spring and summer led to a reduced sum of absolute squared differences between the predicted and observed isotopic signal and consequently to larger NSE-^{18}O values. Moreover, using a free-drainage boundary, the cumulative drainage was reduced significantly by 761 mm during the calibration time. This result clearly demonstrates that using less accurately defined boundary conditions at the top (for example, precipitation) and bottom (free drainage) clearly decreased the ability of the calibrated vadose zone model to simulate water content, matric potential, and drainage.

Table 5. Model performance values from the effective parameterization (Lysimeter), the cross-validation to predict with the effective parameter-set observations from the corresponding single lysimeters (Lys-Wu4, Lys-Wu5, Lys-Wu6, and Lys-Wu8), and the results from simulations using a less accurate measured precipitation (Rain gauge) at the top and free drainage at the bottom. Observation types: water content (NSE-θ), matric potential (NSE-ψ), and $\delta^{18}O$ ratios (NSE-^{18}O); AV-NSE represents model performance for the entire vadose zone and was calculated per lysimeter from single Nash–Sutcliffe efficiency (NSE) values per soil depth and observation type (equally weighted).

Lysimeter	NSE-θ	NSE-ψ	NSE-^{18}O	AV-NSE
Lys-Wu4	−6.30	0.14	0.17	−1.14
Lys-Wu5	−4.65	0.13	0.17	−1.16
Lys-Wu6	−13.84	0.44	−0.14	−3.67
Lys-Wu8	−10.71	0.39	0.50	−3.29
Lysimeter	0.46	0.33	0.02	0.30
Rain gauge	0.37	−45.96	0.29	−16.5

Validation of Dispersivities

The best parameter set obtained for individual lysimeters from the MOS strategy was used to simulate the parallel conducted Br^- tracer experiment in a forward run with HYDRUS-1D for three lysimeters (Lys-Wu4, Lys-Wu6, and Lys-Wu8). Figure 8 plots the Br^- BTCs in four different depths for three lysimeters. Model simulation runs with the lysimeter-specific best parameter set from MOS showed a much faster simulated Br^- breakthrough than the observed breakthrough, particularly at larger depths (see gray dotted lines in Fig. 8). Hence, the simulation results achieved low NSE values, with the exception of Layer 2 (0.1 m).

Bromide has often been used to study the movement of water through the vadose zone due to its presumed conservative properties in most soils (Kasteel et al., 2007; Stumpp et al., 2009; Skaggs et al., 2012). However, a non-conservative behavior (retardation factor $R \neq 1$) of Br^- has been reported in a few studies, where the faster ($R < 1$) or slower ($R > 1$) movement of Br^- than water were attributed to anion exclusion (Gerritse and Adeney, 1992; Russow et al., 1996) or anion adsorption (Boggs and Adams, 1992; Seaman

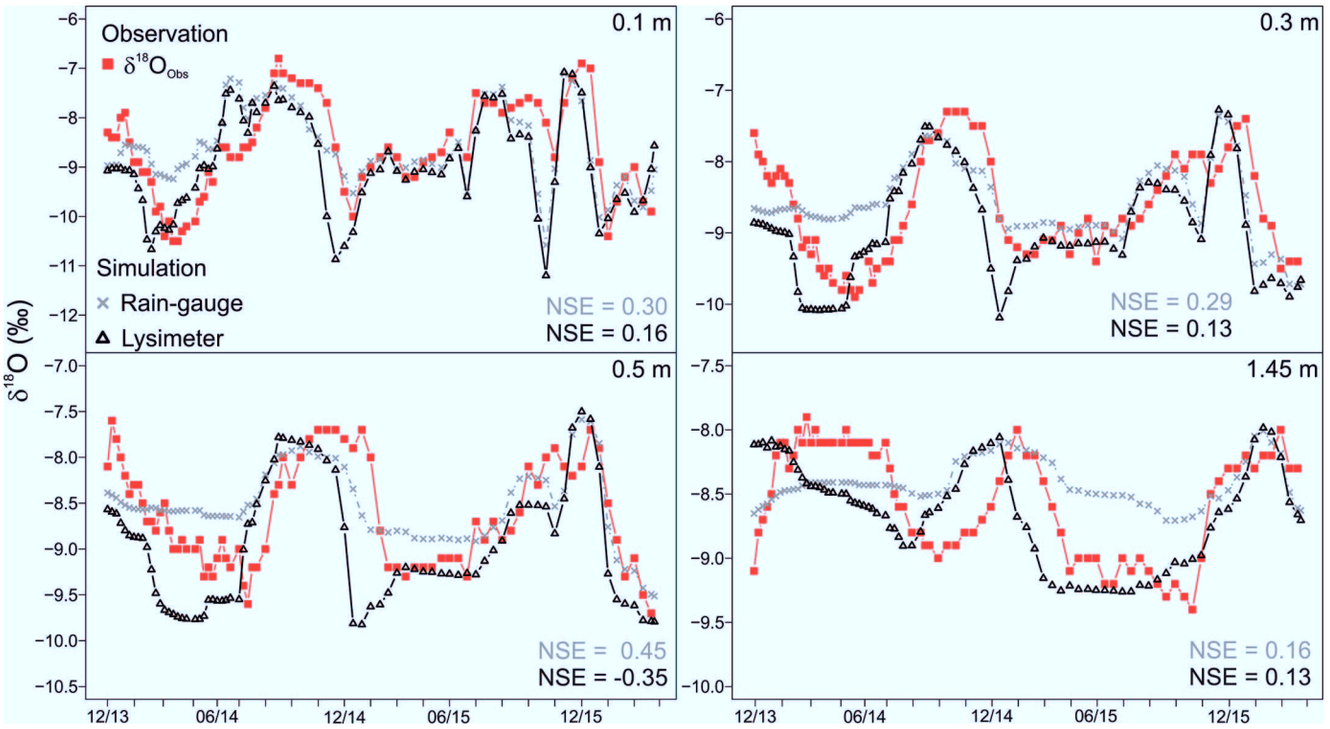

Fig. 7. Observed and simulated $\delta^{18}O$ ratios at four soil depths from simulation runs with upper and lower boundary conditions (i.e., Lysimeter and Rain-gauge, respectively). Nash–Sutcliffe efficiency (NSE) values are also shown.

et al., 1995), respectively. The latter attributed retardation of Br^- in acid soils to adsorption on variably charged minerals (Al and Fe oxides or kaolinite).

The low soil pH values (range 4.2–4.8) and a high availability of oxides (Fe oxides: 2204–16,320 mg kg^{-1}; Mn oxides: 245–6675 mg kg^{-1}; Al oxides: 1412–6980 mg kg^{-1}) suggest that anion adsorption caused the delay of Br^-. We also observed a time lag between the simulated and observed $\delta^{18}O$ time series (for example Lys-Wu4 in 0.5 m, Supplemental Fig. S4). However, these time lags are much smaller and cannot explain the time lag between the observed and simulated Br^- BTCs. When considering adsorption, the simulated Br^- BTC agreed (with the exception of Lys-Wu4 in 0.1 m) much better with observations, particularly at the lysimeter bottom (retardation factors are shown in Fig. 8). Our results of an overall slower movement of Br^- than water in acid soils (pH < 4.8; 0.1 M CaCl) agreed well with previous results from laboratory experiments (Goldberg and Kabengi, 2010). Hence, the use of soil water $\delta^{18}O$ data in our experiment allowed us to identify the non-conservative behavior of Br^- in Wüstebach soils. The mere use of Br^- as a "conservative" tracer under such geochemical conditions would have resulted in clearly different dispersivities and unsaturated hydraulic conductivities than obtained by water stable isotope data ($\delta^{18}O$). Apart from the conservative properties of $\delta^{18}O$, no extra application of tracer is required because it is an environmental tracer, and root water uptake occurs without fractionation (passive). Consequently, water stable isotopes allow monitoring transport behavior in the unsaturated zone for a much longer time period than tracer pulses frequently used in hydrology. Additionally, we demonstrated that an experimental setup with two tracers enables validation of the identified dispersivity parameters based on an independent tracer time series.

Summary and Conclusion

Joint observations of water contents and solute concentrations (Br^-) or isotopic ratios ($\delta^{18}O$, $\delta^{2}H$) have been used in inverse modeling strategies to estimate the soil hydraulic parameters and dispersivities. Our inverse modeling study investigated the possibility of estimating soil hydraulic and dispersivity parameters from observations of water contents and $\delta^{18}O$ ratios that were extended with matric potential measurements in four undisturbed monolithic lysimeters. We evaluated different optimization strategies that considered different combinations of observed variables and sequential vs. simultaneous optimizations. If either water content or matric potential were not included in the optimization, the variable that was not considered could not be reproduced well by the calibration model. This implies that the simulated relation between matric potential and water content, i.e., the water retention curve, did not reproduce the measured relation between the two variables, and the obtained parameters of the retention function were not representative for the soil. When both water content and matric potential were used in the optimization, the simulated and measured water retention curves matched well. A sequential approach in which the transport parameter was fitted using $\delta^{18}O$

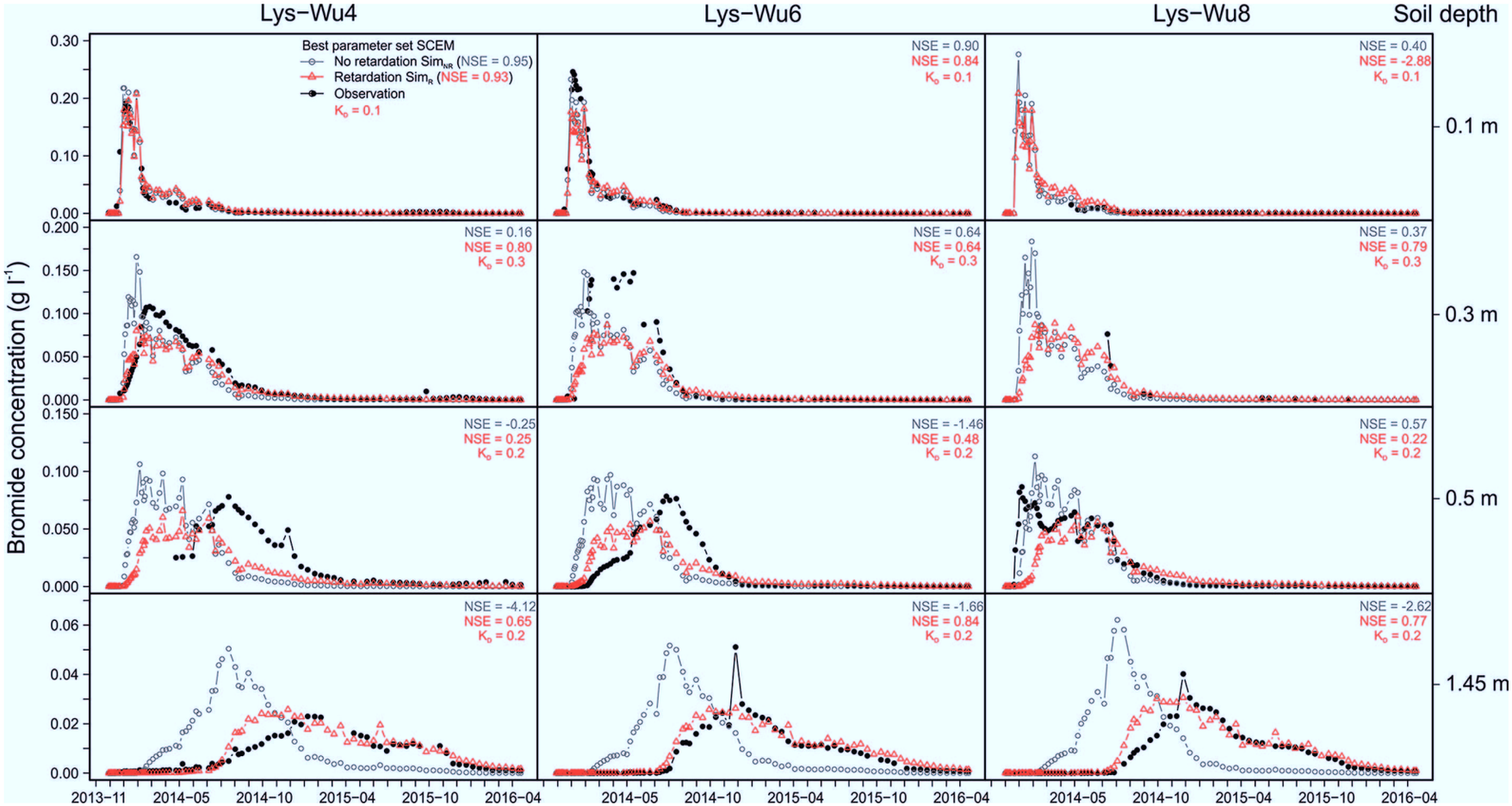

Fig. 8. Observed (black dotted lines) and simulated Br^- tracer breakthrough curves in four different soil depths and for three distinct lysimeters (Lys-Wu4, Lys-Wu6, and Lys-Wu8). Solute transport simulations were conducted with the best parameter from the corresponding multi-objective optimization strategy and a Shuffled Complex Evolution Metropolis (SCEM) algorithm with (red dotted lines) and without (gray dotted lines) solute retardation. K_D is the adsorption isotherm coefficient ($cm^{-3}\ g^{-1}$) and NSE is the Nash–Sutcliffe efficiency.

observations and using soil hydraulic parameters that were fitted based on water content and matric potential observations led to a less good simulation of $\delta^{18}O$ ratios than in the case in which soil hydraulic and the transport parameters were fitted simultaneously. Including $\delta^{18}O$ in the simultaneous optimization led only to a slightly worse simulation of the water content and matric potential than the sequential optimization. This small trade-off indicated that $\delta^{18}O$ observations contained, next to information about transport properties, also information about soil hydraulic properties. Hence, field experiments designed to inverse estimate water flow and solute transport parameters should consider the following points:

- combine water content and matric potential measurements to correctly identify the parameters of the soil water retention curve;
- use water content, matric potential, and tracer data (e.g., $\delta^{18}O$ ratios) simultaneously in the OF during the inverse model calibration to identify soil hydraulic properties and dispersivities of a layered soil.

The water fluxes that were derived at the upper and lower boundary did not vary a lot among the different lysimeters, which suggests that a lysimeter may be considered to be representative of a larger area. However, due to soil heterogeneity, local measurements of state variables vary in space. Considerable variation (particularly in local water content) was observed among the different lysimeters. When local measurements in individual lysimeters are used to parameterize soil properties with the MOS strategy, the obtained water flow and solute transport parameters for a certain layer vary from lysimeter to lysimeter. Still, averaged state variables could be well described using effective parameters, and simulations with these effective parameters reproduced observations of certain state variables in the individual lysimeters fairly well and thus confirmed our assumption that lysimeters are representative of a larger area. The upper and lower boundary conditions derived from lysimeter observations deviated considerably from boundary conditions obtained from other measurement types. Thus, using lysimeter observations to define accurately the boundary conditions of the model domain were highly beneficial and present an important asset of lysimeters. Methods that improve the accuracy of flux measurements in the field, especially precipitation, are therefore central for improving inverse modeling studies. Given the cost of flux measurements in comparison with measurements of water content and matric potential, which can be performed with relatively cheap sensors, saving on these local sensors does not seem economical.

To further confirm our soil profile parameterization, forward simulation runs with the best parameter set using all three state variables (MOS) were evaluated for a parallel Br^- tracer experiment. Field observation of Br^- breakthrough curves showed a clear delay of tracer compared with model simulations. When accounting for anion adsorption on amorphous oxides (Al and Fe) and clay minerals in the acid forest soil (pH < 4.8), the transport of Br^- could be described successfully and hence validated the identified dispersivity parameters independently. Thus, the use of the environmental tracer $\delta^{18}O$ data was beneficial to track water movement through the soil continuously during a relative long time period (2.5 yr) and to confirm the non-conservative behavior of Br^-.

Acknowledgments, Samples, and Data

We acknowledge the support of TERENO and SOILCan, which were funded by the Helmholtz Association (HGF) and the Federal Ministry of Education and Research (BMBF). We want to thank Werner Küpper, Ferdinand Engels, Leander Fürst, and Phillip Meulendick for their great help and work in the field and Martina Krause, Holger Wissel, Andrea Eckert, and Stephanie Stork for supporting the chemical analysis of collected soil water samples. All data for the specific lysimeter and weather station (raw data) can be freely obtained from the TERENO data portal (http://teodoor.icg.kfa-juelich.de/ibg3searchportal2/index.jsp). In addition, we thank our associate editor Lisa Wingate for her constructive comments and three anonymous reviewers for their valuable recommendations.

References

Abbasi, F., J. Šimůnek, J. Feyen, M.Th. van Genuchten, and P.J. Shouse. 2003. Simultaneous inverse estimation of soil hydraulic and solute transport parameters from transient field experiments: Homogeneous soil. Trans. ASAE 46:1085–1095.

Abbaspour, K., R. Kasteel, and R. Schulin. 2000. Inverse parameter estimation in a layered unsaturated field soil. Soil Sci. 165:109–123. doi:10.1097/00010694-200002000-00002

Abdou, H.M., and M. Flury. 2004. Simulation of water flow and solute transport in free-drainage lysimeters and field soils with heterogeneous structures. Eur. J. Soil Sci. 55:229–241. doi:10.1046/j.1365-2389.2004.00592.x

Ad Hoc Arbeitsgruppe Boden. 2005. Bodenkundliche Kartieranleitung. Bundesanstalt für Geowissenschaften und Rohstoffe in Zusammenarbeit mit den Staatlichen Geologischen Diensten, Hannover, Germany.

Aeschbach-Hertig, W., and T. Gleeson. 2012. Regional strategies for the accelerating global problem of groundwater depletion. Nat. Geosci. 5:853–861. doi:10.1038/ngeo1617

Allen, R.G., L.S. Pereira, D. Raes, and M. Smith. 1998. Crop evapotranspiration. Guidelines for computing crop water requirements. Irrig. Drain. Pap. 56. FAO, Rome.

Beven, K. 2006. A manifesto for the equifinality thesis. J. Hydrol. 320:18–36. doi:10.1016/j.jhydrol.2005.07.007

Blok, D., M.M.P.D. Heijmans, G. Schaepman-Strub, J. van Ruijven, F.J.W. Parmentier, T.C. Maximov, and F. Berendse. 2011. The cooling capacity of mosses: Controls on water and energy fluxes in a Siberian tundra site. Ecosystems 14:1055–1065. doi:10.1007/s10021-011-9463-5

Boesten, J.J.T.I. 2007. Simulation of pesticide leaching in the field and in zero-tension lysimeters. Vadose Zone J. 6:793–804. doi:10.2136/vzj2007.0067

Bogena, H., R. Bol, N. Borchard, N. Brüggemann, B. Diekkrüger, C. Drüe, et al. 2015. A terrestrial observatory approach to the integrated investigation of the effects of deforestation on water, energy, and matter fluxes. Sci. China Earth Sci. 58:61–75. doi:10.1007/s11430-014-4911-7

Boggs, J.M., and E.E. Adams. 1992. Field study of dispersion in a heterogeneous aquifer: 4. Investigation of adsorption and sampling bias. Water Resour. Res. 28:3325–3336. doi:10.1029/92WR01759

Borchardt, H. 2012. Einfluss periglazialer Deckschichten auf Abflusssteuerung am Beispiel des anthropogen überprägten Wüstebaches (Nationalpark Eifel). Ph.D. diss. RWTH Aachen, Aachen, Germany.

Butts, M.B., J.T. Payne, M. Kristensen, and H. Madsen. 2004. An evaluation of the impact of model structure on hydrological modelling uncertainty for streamflow simulation. J. Hydrol. 298:242–266. doi:10.1016/j.jhydrol.2004.03.042

Cai, G., J. Vanderborght, V. Couvreur, C.M. Mboh, and H. Vereecken. 2018. Parameterization of root water uptake models considering dynamic root distributions and water uptake compensation. Vadose Zone J. 17:170125 [erratum 17:0201]. doi:10.2136/vzj2016.12.0125

Cai, G., J. Vanderborght, A. Klotzsche, J. van der Kruk, J. Neumann, N. Hermes, and H. Vereecken. 2016. Construction of minirhizotron facilities for investigating root zone processes. Vadose Zone J. 15(9) [erratum 17:170201]. doi:10.2136/vzj2016.05.0043

Caldwell, T.G., T. Wöhling, M.H. Young, D.P. Boyle, and E.V. McDonald. 2013. Characterizing disturbed desert soils using multiobjective parameter optimization. Vadose Zone J. 12(1). doi:10.2136/vzj2012.0083

Crosbie, R.S., W.R. Dawes, S.P. Charles, F.S. Mpelasoka, S. Aryal, O. Barron, and G.K. Summerell. 2011. Differences in future recharge estimates due to GCMs, downscaling methods and hydrological models. Geophys. Res. Lett. 38:L11406. doi:10.1029/2011GL047657

Fang, Z., H. Bogena, S. Kollet, J. Koch, and H. Vereecken. 2015. Spatio-temporal validation of long-term 3D hydrological simulations of a forested catchment using empirical orthogonal functions and wavelet coherence analysis. J. Hydrol. 529:1754–1767. doi:10.1016/j.jhydrol.2015.08.011

Fang, Z., H. Bogena, S. Kollet, and H. Vereecken. 2016. Scale dependent parameterization of soil hydraulic conductivity in 3D simulation of hydrological processes in a forested headwater catchment. J. Hydrol. 536:365–375. doi:10.1016/j.jhydrol.2016.03.020

Fank, J., and G. von Unold. 2007. High-precision weighable field lysimeter: A tool to measure water and solute balance parameters. Int. Water Irrig. 27:28–32.

Feddes, R.A., P.J. Kowalik, and H. Zaradny. 1978. Simulation of field water use and crop yield. John Wiley & Sons, New York.

Flury, M., M.V. Yates, and W.A. Jury. 1999. Numerical analysis of the effect of the lower boundary condition on solute transport in lysimeters. Soil Sci. Soc. Am. J. 63:1493–1499. doi:10.2136/sssaj1999.6361493x

Foolad, F., T.E. Franz, T. Wang, J. Gibson, A. Kilic, R.G. Allen, and A. Suyker. 2017. Feasibility analysis of using inverse modeling for estimating field-scale evapotranspiration in maize and soybean fields from soil water content monitoring networks. Hydrol. Earth Syst. Sci. 21:1263–1277. doi:10.5194/hess-21-1263-2017

Garré, S., M. Javaux, J. Vanderborght, L. Pagès, and H. Vereecken. 2011. Three-dimensional electrical resistivity tomography to monitor root zone water dynamics. Vadose Zone J. 10:412–424. doi:10.2136/vzj2010.0079

Garré, S., J. Koestel, T. Günther, M. Javaux, J. Vanderborght, and H. Vereecken. 2010. Comparison of heterogeneous transport processes observed with electrical resistivity tomography in two soils. Vadose Zone J. 9:336–349. doi:10.2136/vzj2009.0086

Gebler, S., H.J. Hendricks Franssen, T. Pütz, H. Post, M. Schmidt, and H. Vereecken. 2015. Actual evapotranspiration and precipitation measured by lysimeters: A comparison with eddy covariance and tipping bucket. Hydrol. Earth Syst. Sci. 19:2145–2161. doi:10.5194/hess-19-2145-2015

Gerke, H.H., and M.Th. van Genuchten. 1993. A dual-porosity model for simulating the preferential movement of water and solutes in structured porous media. Water Resour. Res. 29:305–319. doi:10.1029/92WR02339

Gerritse, R.G., and J.A. Adeney. 1992. Tracers in recharge: Effects of partitioning in soils. J. Hydrol. 131:255–268. doi:10.1016/0022-1694(92)90221-G

Goldberg, S., and J.N. Kabengi. 2010. Bromide adsorption by reference minerals and soils. Vadose Zone J. 9:780–786. doi:10.2136/vzj2010.0028

Gosling, S.N., R.G. Taylor, N.W. Arnell, and M.C. Todd. 2011. A comparative analysis of projected impacts of climate change on river runoff from global and catchment-scale hydrological models. Hydrol. Earth Syst. Sci. 15:279–294. doi:10.5194/hess-15-279-2011

Groh, J., H. Puhlmann, and K. von Wilpert. 2013. Calibration of a soil-water balance model with a combined objective function for the optimization of the water retention curve. (In German, with English abstract.) Hydrol. Wasserbewirtsch. 57:152–163. doi:10.5675/HyWa_2013,4_1

Groh, J., J. Vanderborght, T. Pütz, and H. Vereecken. 2015. Estimation of evapotranspiration and crop coefficient of an intensively managed grassland ecosystem with lysimeter measurements. In: 16th Gumpensteiner Lysimetertagung, Raumberg-Gumpenstein, Austria. 21–22 Apr. 2015. Höhere Bundeslehr- und Forschungsanstalt für Landwirtschaft, Irdning, Austria. p. 107–112.

Groh, J., J. Vanderborght, T. Pütz, and H. Vereecken. 2016. How to control the lysimeter bottom boundary to investigate the effect of climate change on soil processes? Vadose Zone J. 15(7). doi:10.2136/vzj2015.08.0113

Guo, X., T. Zha, X. Jia, B. Wu, W. Feng, J. Xie, et al. 2016. Dynamics of dew in a cold desert-shrub ecosystem and its abiotic controls. Atmosphere 7(3):32. doi:10.3390/atmos7030032

Hagenau, J., R. Meissner, and H. Borg. 2015. Effect of exposure on the water balance of two identical lysimeters. J. Hydrol. 520:69–74. doi:10.1016/j.jhydrol.2014.11.030

Hannes, M., U. Wollschläger, F. Schrader, W. Durner, S. Gebler, T. Pütz, et al. 2015. A comprehensive filtering scheme for high-resolution estimation of the water balance components from high-precision lysimeters. Hydrol. Earth Syst. Sci. 19:3405–3418. doi:10.5194/hess-19-3405-2015

Heimovaara, T.J., J.A. Huisman, J.A. Vrugt, and W. Bouten. 2004. Obtaining the spatial distribution of water content along a TDR probe using the SCEM-UA Bayesian inverse modeling scheme. Vadose Zone J. 3:1128–1145. doi:10.2136/vzj2004.1128

Herbrich, M., H.H. Gerke, O. Bens, and M. Sommer. 2017. Water balance and leaching of dissolved organic and inorganic carbon of eroded Luvisols using high precision weighing lysimeters. Soil Tillage Res. 165:144–160. doi:10.1016/j.still.2016.08.003

Heusinger, J., and S. Weber. 2015. Comparative microclimate and dewfall measurements at an urban green roof versus bitumen roof. Build. Environ. 92:713–723. doi:10.1016/j.buildenv.2015.06.002

Hoffmann, M., R. Schwartengräber, G. Wessolek, and A. Peters. 2016. Comparison of simple rain gauge measurements with precision lysimeter data. Atmos. Res. 174–175:120–123. doi:10.1016/j.atmosres.2016.01.016

Hopmans, J.W., D.R. Nielsen, and K.L. Bristow. 2013. How useful are small-scale soil hydraulic property measurements for large-scale vadose zone modeling? In: P.A.C. Raats et al., editors, Environmental mechanics: Water, mass and energy transfer in the biosphere (The Philip volume). Geophys. Monogr. Ser. 129. Am. Geophys. Union, Washington, DC. p. 247–258.

Huang, M., J.N. Hilderman, and L. Barbour. 2015. Transport of stable isotopes of water and sulphate within reclaimed oil sands saline–sodic mine overburden. J. Hydrol. 529:1550–1561. doi:10.1016/j.jhydrol.2015.08.028

Iiyama, I. 2016. Differences between field-monitored and laboratory-measured soil moisture characteristics. Soil Sci. Plant Nutr. 62:416–422. doi:10.1080/00380768.2016.1242367

Jacques, D., J. Šimůnek, A. Timmerman, and J. Feyen. 2002. Calibration of Richards' and convection–dispersion equations to field-scale water flow and solute transport under rainfall conditions. J. Hydrol. 259:15–31. doi:10.1016/S0022-1694(01)00591-1

Jarvis, N. 1994. The MACRO model (version 3.1): Technical description and sample simulations. Rep. Diss. 19. Dep. of Soil Sci., Swedish Univ. of Agric. Sci., Uppsala, Sweden.

Kasteel, R., T. Pütz, and H. Vereecken. 2007. An experimental and numerical study on flow and transport in a field soil using zero-tension lysimeters and suction plates. Eur. J. Soil Sci. 58:632–645. doi:10.1111/j.1365-2389.2006.00850.x

Knauer, N., J. Groh, H. Vereecken, and T. Pütz. 2017. Veränderungen des Stickstoff-Haushaltes eines Waldwiesen-Standortes durch den Klimawandel. In: 17th Gumpensteiner Lysimetertagung, Raumberg-Gumpenstein, Austria. 9–10 May 2017. Höhere Bundeslehr- und Forschungsanstalt für Landwirtschaft, Irdning, Austria. p. 93–102.

Koestel, J., J. Vanderborght, M. Javaux, A. Kemna, A. Binley, and H. Vereecken. 2009a. Noninvasive 3-D transport characterization in a sandy soil using ERT: 1. Investigating the validity of ERT-derived transport parameters. Vadose Zone J. 8:711–722. doi:10.2136/vzj2008.0027

Koestel, J., J. Vanderborght, M. Javaux, A. Kemna, A. Binley, and H. Vereecken. 2009b. Noninvasive 3-D transport characterization in a sandy soil using ERT: 2. Transport process. Vadose Zone J. 8:723–734. doi:10.2136/vzj2008.0154

Korres, W., T.G. Reichenau, P. Fiener, C.N. Koyama, H.R. Bogena, T. Cornelissen, et al. 2015. Spatio-temporal soil moisture patterns: A meta-analysis using plot to catchment scale data. J. Hydrol. 520:326–341. doi:10.1016/j.jhydrol.2014.11.042

Kung, K.-J.S. 1990. Influence of plant uptake on the performance of bromide tracer. Soil Sci. Soc. Am. J. 54:975–979. doi:10.2136/sssaj1990.03615995005400040006x

Küpper, W., J. Groh, L. Fürst, P. Meulendick, H. Vereecken, and T. Pütz. 2017. TERENO-SOILCan-Management eines deutschlandweiten Lysimeternetzwerkes. In: 17th Gumpensteiner Lysimetertagung, Raumberg-Gumpenstein, Austria. 9–10 May 2017. Höhere Bundeslehr- und Forschungsanstalt für Landwirtschaft, Irdning, Austria. p. 175–180.

Lai, J., and L. Ren. 2016. Estimation of effective hydraulic parameters in heterogeneous soils at field scale. Geoderma 264:28–41. doi:10.1016/j.geoderma.2015.09.013

Le Bourgeois, O., C. Bouvier, P. Brunet, and P.A. Ayral. 2016. Inverse modeling of soil water content to estimate the hydraulic properties of a shallow soil and the associated weathered bedrock. J. Hydrol. 541:116–126. doi:10.1016/j.jhydrol.2016.01.067

Li, H., L. Luo, E.F. Wood, and J. Schaake. 2009. The role of initial conditions and forcing uncertainties in seasonal hydrologic forecasting. J. Geophys. Res.114:D04114. doi:10.1029/2008JD010969

Magarian, D.M., M.P. Russelle, J.F.S. Lamb, and J.M. Blumenthal. 1998. Bromide as a tracer for nitrate-N uptake in alfalfa herbage. Agron. J. 90:651–657. doi:10.2134/agronj1998.00021962009000050014x

Mannschatz, T., and P. Dietrich. 2017. Model input data uncertainty and its potential impact on soil properties. In: G. Petropoulos and P.K. Srivastava, editors, Sensitivity analysis in earth observation modelling. Elsevier, Amsterdam. p. 25–52.

McCarter, C.P.R., and J.S. Price. 2014. Ecohydrology of *Sphagnum* moss hummocks: Mechanisms of capitula water supply and simulated effects of evaporation. Ecohydrology 7:33–44. doi:10.1002/eco.1313

Mertens, J., H. Madsen, M. Kristensen, D. Jacques, and J. Feyen. 2005. Sensitivity of soil parameters in unsaturated zone modelling and the relation between effective, laboratory and in situ estimates. Hydrol. Processes 19:1611–1633. doi:10.1002/hyp.5591

Mishra, S., and J.C. Parker. 1989. Parameter estimation for coupled unsaturated flow and transport. Water Resour. Res. 25:385–396. doi:10.1029/WR025i003p00385

Moeck, C., P. Brunner, and D. Hunkeler. 2016. The influence of model structure on groundwater recharge rates in climate-change impact studies. Hydrogeol. J. 24:1171–1184. doi:10.1007/s10040-016-1367-1

Monteith, J.L., and M.H. Unsworth. 1990. Principles of environmental physics. 2nd ed. Edward Arnold, London.

Mualem, Y. 1976. A new model for predicting the hydraulic conductivity of unsaturated porous media. Water Resour. Res. 12:513–522. doi:10.1029/WR012i003p00513

Peters, A., and W. Durner. 2006. Improved estimation of soil water retention characteristics from hydrostatic column experiments. Water Resour. Res. 42:W11401. doi:10.1029/2006WR004952

Peters, A., and W. Durner. 2008. Simplified evaporation method for determining soil hydraulic properties. J. Hydrol. 356:147–162. doi:10.1016/j.jhydrol.2008.04.016

Peters, A., W. Durner, and G. Wessolek. 2011. Consistent parameter constraints for soil hydraulic functions. Adv. Water Resour. 34:1352–1365. doi:10.1016/j.advwatres.2011.07.006

Peters, A., J. Groh, F. Schrader, W. Durner, H. Vereecken, and T. Pütz. 2017. Towards an unbiased filter routine to determine precipitation and evapotranspiration from high precision lysimeter measurements. J. Hydrol. 549:731–740. doi:10.1016/j.jhydrol.2017.04.015

Peters, A., S.C. Iden, and W. Durner. 2015. Revisiting the simplified evaporation method: Identification of hydraulic functions considering vapor, film and corner flow. J. Hydrol. 527:531–542. doi:10.1016/j.jhydrol.2015.05.020

Peters-Lidard, C.D., D.M. Mocko, M. Garcia, J.A. Santanello, Jr., M.A. Tischler, M.S. Moran, and Y. Wu. 2008. Role of precipitation uncertainty in the estimation of hydrologic soil properties using remotely sensed soil moisture in a semiarid environment. Water Resour. Res. 44:W05S18. doi:10.1029/2007WR005884

Price, J.S., and P.N. Whittington. 2010. Water flow in *Sphagnum* hummocks: Mesocosm measurements and modelling. J. Hydrol. 381:333–340. doi:10.1016/j.jhydrol.2009.12.006

Puhlmann, H., and K. von Wilpert. 2012. Pedotransfer functions for water retention and unsaturated hydraulic conductivity of forest soils. J. Plant Nutr. Soil Sci. 175:221–235. doi:10.1002/jpln.201100139

Pütz, T., R. Kiese, U. Wollschläger, J. Groh, H. Rupp, S. Zacharias, et al. 2016. TERENO-SOILCan: A lysimeter-network in Germany observing soil processes and plant diversity influenced by climate change. Environ. Earth Sci. 75:1242. doi:10.1007/s12665-016-6031-5

Qu, W., H.R. Bogena, J.A. Huisman, G. Martinez, Y.A. Pachepsky and H. Vereecken. 2014. Effects of soil hydraulic properties on the spatial variability of soil water content: Evidence from sensor network data and inverse modeling. Vadose Zone J. 13(12). doi:10.2136/vzj2014.07.0099

Raat, K.J., J.A. Vrugt, W. Bouten, and A. Tietema. 2004. Towards reduced uncertainty in catchment nitrogen modelling: Quantifying the effect of field observation uncertainty on model calibration. Hydrol. Earth Syst. Sci. 8:751–763. doi:10.5194/hess-8-751-2004

Richter, D. 1995. Results of methodological studies on the correction of the systematic measurement error of the Hellmann-type precipitation gauge. (In German.) German Weather Serv., Offenbach am Main.

Ries, F., J. Lange, S. Schmidt, H. Puhlmann, and M. Sauter. 2015. Recharge estimation and soil moisture dynamics in a Mediterranean, semi-arid karst region. Hydrol. Earth Syst. Sci. 19:1439–1456. doi:10.5194/hess-19-1439-2015

Romano, N., and P. Nasta. 2016. How effective is bimodal soil hydraulic characterization? Functional evaluations for predictions of soil water balance. Eur. J. Soil Sci. 67:523–535. doi:10.1111/ejss.12354

Rosenbaum, U., H.R. Bogena, M. Herbst, J.A. Huisman, T.J. Peterson, A. Weuthen, et al. 2012. Seasonal and event dynamics of spatial soil moisture patterns at the small catchment scale. Water Resour. Res. 48:W10544. doi:10.1029/2011WR011518

Russow, R., H. Segschneider, and H. Förstel. 1996. Vergleich der Wasser- und Anionenbewegung in agrarisch genutzten Sandlöss- und Löss-Schwarzerde-Böden an Hand von Multitracer-Untersuchungen. Arch. Acker- Pflanzenbau Bodenkd. 40:453–471. doi:10.1080/03650349609365972

Schaap, M.G., and F.J. Leij. 2000. Improved prediction of unsaturated hydraulic conductivity with the Mualem–van Genuchten model. Soil Sci. Soc. Am. J. 64:843–851. doi:10.2136/sssaj2000.643843x

Scharnagl, B., J.A. Vrugt, H. Vereecken, and M. Herbst. 2011. Inverse modelling of in situ soil water dynamics: Investigating the effect of different prior distributions of the soil hydraulic parameters. Hydrol. Earth Syst. Sci. 15:3043–3059. doi:10.5194/hess-15-3043-2011

Schelle, H., W. Durner, S.C. Iden, and J. Fank. 2013. Simultaneous estimation of soil hydraulic and root distribution parameters from lysimeter data by inverse modeling. Procedia Environ. Sci. 19:564–573. doi:10.1016/j.proenv.2013.06.064

Schelle, H., S.C. Iden, J. Fank, and W. Durner. 2012. Inverse estimation of soil hydraulic and root distribution parameters from lysimeter data. Vadose Zone J. 11(4). doi:10.2136/vzj2011.0169

Schnabel, R.R., W.L. Stout, and J.A. Shaffer. 1995. Uptake of a hydrologic tracer (bromide) by ryegrass from well and poorly-drained soils. J. Environ. Qual. 24:888–892. doi:10.2134/jeq1995.00472425002400050015x

Schrader, F., W. Durner, J. Fank, S. Gebler, T. Pütz, M. Hannes, and U. Wollschläger. 2013. Estimating precipitation and actual evapotranspiration from precision lysimeter measurements. Procedia Environ. Sci. 19:543–552. doi:10.1016/j.proenv.2013.06.061

Schwaerzel, K., and H.P. Bohl. 2003. An easily installable groundwater lysimeter to determine waterbalance components and hydraulic properties of peat soils. Hydrol. Earth Syst. Sci. 7:23–32. doi:10.5194/hess-7-23-2003

Seaman, J.C., P.M. Bertsch, and W.P. Miller. 1995. Ionic tracer movement through highly weathered sediments. J. Contam. Hydrol. 20:127–143. doi:10.1016/0169-7722(95)00043-U

Seki, K., P. Ackerer, and F. Lehmann. 2015. Sequential estimation of hydraulic parameters in layered soil using limited data. Geoderma 247–248:117–128. doi:10.1016/j.geoderma.2015.02.013

Šimůnek, J., M. Šejna, H. Saito, M. Sakai, and M.Th. van Genuchten. 2013. The HYDRUS-1D software package for simulating the movement of water, heat, and multiple solutes in variably saturated media. Version 4.16. HYDRUS Softw. Ser. 3. Dep. of Environ. Sci., Univ. of California, Riverside.

Šimůnek, J., M.Th. van Genuchten, and M. Šejna. 2016. Recent developments and applications of the HYDRUS computer software packages. Vadose Zone J. 15(7). doi:10.2136/vzj2016.04.0033

Skaggs, T.H., D.L. Suarez, S. Goldberg, and P.J. Shouse. 2012. Replicated lysimeter measurements of tracer transport in clayey soils: Effects of irrigation water salinity. Agric. Water Manage. 110:84–93. doi:10.1016/j.agwat.2012.04.003

Sprenger, M., M. Erhardt, M. Riedel, and M. Weiler. 2016a. Historical tracking of nitrate in contrasting vineyards using water isotopes and nitrate depth profiles. Agric. Ecosyst. Environ. 222:185–192. doi:10.1016/j.agee.2016.02.014

Sprenger, M., S. Seeger, T. Blume and M. Weiler. 2016b. Travel times in the vadose zone: Variability in space and time. Water Resour. Res. 52:5727–5754. doi:10.1002/2015WR018077

Sprenger, M., T.H.M. Volkmann, T. Blume, and M. Weiler. 2015. Estimating flow and transport parameters in the unsaturated zone with pore water stable isotopes. Hydrol. Earth Syst. Sci. 19:2617–2635. doi:10.5194/hess-19-2617-2015

Stenitzer, E., and J. Fank. 2007. "Tension-free" lysimeters versus "controlled tension" lysimeters: A simulation study. In: Proceedings of the Conference Diffuse Inputs into Groundwater: Monitoring, Modelling, Management, Graz, Austria. 29–31 Jan. 2007. Joanneum Redearch, Graz. p. 149–152.

Stockinger, M.P., H.R. Bogena, A. Lücke, B. Diekkrüger, T. Cornelissen, and H. Vereecken. 2016. Tracer sampling frequency influences estimates of young water fraction and streamwater transit time distribution. J. Hydrol. 541:952–964. doi:10.1016/j.jhydrol.2016.08.007

Stockinger, M.P., A. Lücke, J.J. McDonnell, B. Diekkrüger, H. Vereecken, and H.R. Bogena. 2015. Interception effects on stable isotope driven streamwater transit time estimates. Geophys. Res. Lett. 42:5299–5308. doi:10.1002/2015GL064622

Stofberg, S.F., J. van Engelen, J.-P.M. Witte, and S.E.A.T.M. van der Zee. 2016. Effects of root mat buoyancy and heterogeneity on floating fen hydrology. Ecohydrology 9:1222–1234. doi:10.1002/eco.1720

Stumpp, C., G. Nützmann, S. Maciejewski, and P. Maloszewski. 2009. A comparative modeling study of a dual tracer experiment in a large lysimeter under atmospheric conditions. J. Hydrol. 375:566–577. doi:10.1016/j.jhydrol.2009.07.010

Stumpp, C., W. Stichler, M. Kandolf, and J. Šimůnek. 2012. Effects of land cover and fertilization method on water flow and solute transport in five lysimeters: A long-term study using stable water isotopes. Vadose Zone J. 11(1). doi:10.2136/vzj2011.0075

Suzuki, K., J. Kubota, H. Yabuki, T. Ohata, and V. Vuglinsky. 2007. Moss beneath a leafless larch canopy: Influence on water and energy balances in the southern mountainous taiga of eastern Siberia. Hydrol. Processes 21:1982–1991. doi:10.1002/hyp.6709

Taylor, R.G., B. Scanlon, P. Doll, M. Rodell, R. van Beek, Y. Wada, et al. 2013. Ground water and climate change. Nat. Clim. Change 3:322–329. doi:10.1038/nclimate1744

Vanderborght, J., and H. Vereecken. 2007. Review of dispersivities for transport modeling in soils. Vadose Zone J. 6:29–52. doi:10.2136/vzj2006.0096

van Genuchten, M.Th. 1980. A closed-form equation for predicting the hydraulic conductivity of unsaturated soils. Soil Sci. Soc. Am. J. 44:892–898. doi:10.2136/sssaj1980.03615995004400050002x

van Genuchten, M.Th., F.J. Leij, and S.R. Yates. 1991. The RETC code for quantifying the hydraulic functions of unsaturated soils. Version 1.0. US Salinity Lab. Riverside, CA.

Vereecken, H., J.A. Huisman, H. Bogena, J. Vanderborght, J.A. Vrugt, and J.W. Hopmans. 2008. On the value of soil moisture measurements in vadose zone hydrology: A review. Water Resour. Res. 44:W00D06. doi:10.1029/2008WR006829

von Unold, G., and J. Fank. 2008. Modular design of field lysimeters for specific application needs. Water Air Soil Pollut. Focus 8:233–242. doi:10.1007/s11267-007-9172-4

Vrugt, J.A., H.V. Gupta, W. Bouten, and S. Sorooshian. 2003. A Shuffled Complex Evolution Metropolis algorithm for optimization and uncertainty assessment of hydrologic model parameters. Water Resour. Res. 39:1201. doi:10.1029/2002WR001642

Vrugt, J.A., P.H. Stauffer, T. Wöhling, B.A. Robinson, and V.V. Vesselinov. 2008. Inverse modeling of subsurface flow and transport properties: A review with new developments. Vadose Zone J. 7:843–864. doi:10.2136/vzj2007.0078

Werisch, S., J. Grundmann, H. Al-Dhuhli, E. Algharibi, and F. Lennartz. 2014. Multiobjective parameter estimation of hydraulic properties for a sandy soil in Oman. Environ. Earth Sci. 72:4935–4956. doi:10.1007/s12665-014-3537-6

Wiekenkamp, I., J.A. Huisman, H.R. Bogena, H.S. Lin, and H. Vereecken. 2016. Spatial and temporal occurrence of preferential flow in a forested headwater catchment. J. Hydrol. 534:139–149. doi:10.1016/j.jhydrol.2015.12.050

Wöhling, T., and J.A. Vrugt. 2011. Multiresponse multilayer vadose zone model calibration using Markov chain Monte Carlo simulation and field water retention data. Water Resour. Res. 47:W04510. doi:10.1029/2010WR009265

Wöhling, T., J.A. Vrugt, and G.F. Barkle. 2008. Comparison of three multiobjective optimization algorithms for inverse modeling of vadose zone hydraulic properties. Soil Sci. Soc. Am. J. 72:305–319. doi:10.2136/sssaj2007.0176

Xiao, H., R. Meissner, J. Seeger, H. Rupp, and H. Borg. 2009. Effect of vegetation type and growth stage on dewfall, determined with high precision weighing lysimeters at a site in northern Germany. J. Hydrol. 377:43–49. doi:10.1016/j.jhydrol.2009.08.006

Xu, S., A.C. Leri, S.C.B. Myneni, and P.R. Jaffé. 2004. Uptake of bromide by two wetland plants (*Typha latifolia* L. and *Phragmites australis* (Cav.) Trin. ex Steud). Environ. Sci. Technol. 38:5642–5648. doi:10.1021/es049568o

Zhang, Z.F., A.L. Ward, and G.W. Gee. 2003. Estimating soil hydraulic parameters of a field drainage experiment using inverse techniques. Vadose Zone J. 2:201–211. doi:10.2136/vzj2003.2010